行政院國家科學委員會專題研究計畫　期中進度報告

轉錄因子 C1EBPα及 C1EBPβ isoforms 在脂肪細胞分化所扮演的角色：不同階段的活化與對不同基因的調控機轉(2/3)

計畫類別： 個別型計畫
計畫編號： NSC93-2320-B-002-105-
執行期間： 93 年 08 月 01 日至 94 年 07 月 31 日
執行單位： 國立臺灣大學醫學院分子醫學研究所

計畫主持人： 呂勝春

報告類型： 精簡報告

處理方式： 本計畫可公開查詢

中　華　民　國 94 年 6 月 8 日

Functional cooperation between FACT and the MCM helicase complex facilitates chromatin DNA replication

Bertrand Chin-Ming Tan,[1] Cheng-Ting Chien,[2] Susumu Hirose,[4] and Sheng-Chung Lee[1,3,*]

[1]Institute of Molecular Medicine and Institute of Clinical Medicine, National Taiwan University, Taipei, Taiwan
[2]Institute of Molecular Biology, and [3]Institute of Biological Chemistry, Academia Sinica, Taipei, Taiwan
[4]Department of Developmental Genetics, National Institute of Genetics, 1111 Yata, Mishima, Shizuokaken 411-8540, Japan

Summary

Chromatin is suppressive in nature to cellular enzymes that metabolize DNA, mainly due to the inherent inaccessibility of the DNA template. Despite extensive understanding of the involvement of chromatin-modifying factors in transcription, role of related activities in DNA replication remains largely elusive. Here we show that the transcription elongation factor FACT is functionally linked to DNA synthesis progression. Its involvement in DNA replication is partly mediated by the stable association with the replicative helicase complex, MCM, and further by the coexistence with MCM on replication origin. Furthermore, reliant on its nucleosome-reorganizing activity, FACT possesses the ability to facilitate chromatin unwinding by the MCM complex, which is otherwise inert on the nucleosomal template. As a consequence, FACT positively regulates DNA replication and S phase progression *in vivo*, and such replicative role is evolutionarily conserved. Together, our findings identify FACT as an integral and conserved component of the endogenous replication machinery, and further outline a model in which the concerted action of helicase and chromatin-modifying activities promotes chromatin replication.

Running Title

The FACT-MCM complex facilitates DNA replication

Introduction

Macromolecular interactions of multiprotein complexes underlie cellular execution of highly regulated processes. DNA replication is one such event, occurrence of which must be temporally restricted to prevent catastrophic aberration of the genome. Ordered assembly of various replication initiation/licensing factors

(ORCs, CDT1, CDC6, and MCM2-7) onto the origins constitutes a conserved initiation mechanism (Bell and Dutta, 2002; Kelly and Brown, 2000). Ensuing protein phosphorylation by kinase leads to origin firing and coordinates DNA replication with cell cycle progression (Bell and Dutta, 2002; Masai and Arai, 2002; Tanaka et al., 1997). Upon recruitment of additional initiation factors and polymerases, bi-directional DNA synthesis proceeds in the form of replication forks (reviewed in Bell and Dutta, 2002). Among the different replication factors, the hexameric helicase complex MCM provides an essential activity that has been directly implicated in both the initiation and elongation steps. Chromatin immunoprecipitation (ChIP) assays and conditional mutant analysis done in *S. cerevisiae* have pinpointed the association and a requisite role of all six MCM subunits in replication fork movement (Aparicio et al., 1997; Labib et al., 2000). Catalytically, the ATP-hydrolyzing and DNA unwinding activities have been demonstrated for distinct subcomplexes of MCM but not the heterohexamer (Davey et al., 2003; Ishimi, 1997; Lee and Hurwitz, 2000; Lee and Hurwitz, 2001; You et al., 1999). Work done by Schwacha and Bell further discriminated two functionally distinct Mcm protein subgroups: Mcm4/6/7p comprises the "catalytic core", while Mcm2/3/5p serves a regulatory function (Schwacha and Bell, 2001). These results suggest that distinct assembly of subcomplexes among the MCM subunits may contribute to the coordinated or differential actions during the progression of replication.

Analogous to transcription, the progression of DNA replication must overcome the structural hindrance imposed by the nucleosomal template. Although the molecular basis of chromatin on this process is presently not clear, several lines of evidence have demonstrated that local chromatin environment indeed dictates origin activity. First, early studies on the yeast ARS1 origin revealed that the origin is located in a nucleosome-free region. Forced positioning of nucleosome on origin element markedly reduced ORC binding as well as replication efficiency, underscoring the negative role of chromatin structure (Bell and Dutta, 2002; Gillespie and Blow, 2000; Simpson, 1990). Second, a link between the degree of chromatin packaging and the selective usage of origin has been observed. Temporal activation of origins (early vs. late) was found in association with transcription profile, state of local chromatin structure, and nuclear architecture (Gilbert et al., 1995; Hyrien et al., 1997; Hyrien et al., 1995). Finally, recent reports have pinpointed a direct association of chromatin acetylation with active origins. Work done on the origin sequence within the terminal repeats of the Kaposi's sarcoma-associated herpevirus genome (Stedman et al., 2004) as well as on the chorion locus origin in *Drosophila* somatic follicle cells (Aggarwal and Calvi, 2004) both demonstrated a specific enrichment in hyperacetylated histones H3 and H4 and/or a S phase-specific loss of H3 K4

methylation. These findings further emphasize the unique chromatin context that origin resides and a direct role of epigenetic determinants in DNA replication. Based on these experimental observations, it is conceivable that, comparable to the myriad of chromatin modulating and modifying activities associated with transcription, distinct or overlapping sets of chromatin-specific factors might exist to facilitate chromatin replication. Indeed, interaction of a histone acetyltransferase HBO1 with the replication apparatus was previously reported (Burke et al., 2001; Iizuka and Stillman, 1999). The chromatin accessibility complex (CHRAC) was also identified as the ATP-dependent cofactor that mediates replication *in vitro* from a nucleosome-covered SV40 origin by altering nucleosomal structure at origin and allowing binding of T-antigen (Alexiadis et al., 1998). However, direct involvement of these factors in chromatin replication *in vivo* has not been demonstrated.

The FACT (facilitates chromatin transcription) complex, a heterodimer of hSpt16 and SSRP1 proteins, represents another class of chromatin structure modulator whose replicative function has preliminarily been reported. Initially identified as an elongation factor that facilitate transcription of nucleosomal templates *in vitro* (LeRoy et al., 1998; Orphanides et al., 1998; Orphanides et al., 1999), FACT is now known to reorganize nucleosomal structure presumably by removal and/or reassembly of the histone H2A-H2B dimers (Belotserkovskaya et al., 2003). The pleiotropic nature of FACT's functions is illustrated by the reported involvement in replication, transcription, and even DNA repair (Keller and Lu, 2002; Keller et al., 2001). These reports support the notion that FACT acts as a core activity that, when in conjunction with pathway-specific cofactors, mediates chromatin loosening during the progression of different DNA-metabolizing events.

The role of FACT in DNA replication was well documented by studies on the yeast and *Xenopus* FACT homologues (Spt16/Pob3 and DUF, respectively). DUF was shown to possess the ability to replicate exogenously added sperm nuclei or plasmid DNA (Okuhara et al., 1999). Mutation in the yeast Pob3 gene led to delayed S phase progression (Schlesinger and Formosa, 2000). The involvement of yFACT in DNA replication was further supported by its interaction with DNA polymerase α (Wittmeyer and Formosa, 1997; Wittmeyer et al., 1999) and genetic interactions with genes encoding DNA replication factors POL1, CTF4, DNA2, and CHL12 (Schlesinger and Formosa, 2000). However, the molecular mechanism underlying the replicative functions of DUF and yFACT, as well as the functional link between human FACT and DNA replication have not been substantiated.

In the present study, we show that like its yeast counterpart, human FACT is essential for proper progression of DNA synthesis. We identified the MCM complexes as novel interacting proteins of the FACT heterodimer, thus providing a basis for

FACT's involvement in DNA replication. We further analyzed the physical and functional interactions between FACT and MCM. Our data demonstrate that the conserved replicative role of FACT potentially lies in its ability to facilitate chromatin unwinding by the MCM complex.

Results

Identification of the MCM complex as a novel interacting partner of FACT

As a means to probe the underlying basis of FACT's cellular role, we examined the constituents of the FACT-associated complexes. Using a proteomic approach described previously (Tan and Lee, 2004), we identified through anti-SSRP1 monoclonal antibody (clone 10D1) immunoprecipitation and mass spectrometric analysis two subunits of the replicative helicase complex MCM, MCM4 and MCM6, as novel interacting partners of FACT (Figure 1A).

MCM complexes normally exist in multimeric form. However, the apparent absence of additional MCM components (other than MCM4 and MCM6) in the FACT immunoprecipitates, as judged by the silver stained gel and mass spectrometric results, does not quite reflect such composite nature. Thus, to achieve a more sensitive and accurate detection, we performed Western blot analysis on anti-FACT immunoprecipitates isolated from whole cell extracts (Figure 1B). The presence of MCM4 and MCM6 in the 10D1-targeted complex was first confirmed by the respective specific antibody (Figure 1B, bottom panel; data not shown). Interestingly, by using different antibodies that recognize pan or individual MCM subunits, we discovered that additional MCM proteins, MCM2 and MCM7, are associated with the 10D1 precipitates (Figure 1B, middle panel; Figure 1D, bottom panel). On the other hand, coprecipitation of MCM3 and MCM5 was not observed by Western blot or mass spectrometry (data not shown). These results demonstrate that FACT may interact with a discrete subcomplex of the MCM proteins. Conversely, endogenous FACT heterodimer was specifically detected in the MCM complexes pulled down by an anti-MCM4 antibody (Figure 1C). As controls, the pre-immune sera and an anti-MCM3 antibody, which only minimally precipitated MCM3, did not coprecipitate FACT. Partial co-localization between FACT and MCM4 in the nucleus can also be readily detected (data not shown). (This sentence may be deleted!)

Next, we subjected HeLa nuclear extracts (Figure 1D) to gel filtration to further verify the presence of FACT-MCM complexes. As shown by Western blot, both FACT and MCM subunits have broad and overlapping distributions in fractions ranging in molecular size from 669 kDa to 2 MDa (Figure 1D, top panel). To further distinguish the physical association between the FACT and MCM subcomplexes, we subjected gel filtration fractions to immunoprecipitation. Presence of the MCM2/4/6/7 subunits

in the 10D1 immunoprecipitates from fractions 8-32 confirms the coelution of these two complexes and suggests that they combine to form complexes of various sizes (Figure 1D and data not shown). Furthermore, this immunoprecipitation assay approximately resolved two different peaks of co-purified MCMs. The molecular sizes of the peak 2 immunocomplexes (~700 kDa) are consistent with a heterohexameric composition of FACT and MCM2/4/6/7. The true identity of the immunocomplexes in peak 1 fractions cannot be deduced by our experiment. Yet, our results do not preclude the existence of additional, higher molecular-weight FACT-MCM complexes (in the MDa range) that might either be multimers or include other interacting polypeptides or DNA. The interaction between FACT and MCM is genuinely DNA-independent, however, as indicated by the intactness of the immunocomplexes under nuclease treatment (data not shown).

We further characterized the specific interaction between these two complexes. First, to exclude the possibility that FACT and MCMs are bridged by a third protein(s), we tested the *in vitro* association of these two complexes. Purified preparations of the MCM2/4/6/7 heterotetramer and the recombinant FLAG-hSpt16/His_6-SSRP1 heterodimer (Figure 1E, upper two panels; see Materials and Methods) were subjected to *in vitro* binding assay using the M2 agarose. We subsequently found that the MCM complex could be specifically detected in the co-precipitates (Figure 1E, lower panel), indicating a direct interaction between complexes. Second, in an *in vitro* pull-down assay using GST-fused recombinant MCM subunit proteins, both FLAG-hSpt16p and His_6-SSRP1 were found to bind GST-MCM4 only (Figure 1F). Furthermore, distinct and even multiple regions (as in the case of SSRP1) of the MCM4 polypeptide may be involved in such binding (Figure 1F). Accordingly, down-regulation of MCM4 expression by RNAi (Figure 1G) or co-incubation with an interaction domain-containing MCM4 fragment (GST-$MCM4_{1-250}$, encompassing the first 250 amino acids) (Figure 1H) both led to disruption of the FACT-MCM immunocomplexes *in vivo* and *in vitro*, respectively. Taken together, these data show a specific physical interaction between FACT and MCM2/4/6/7 and that the complex formation is mediated by contact of MCM4 with both FACT subunits.

The catalytic activity of the FACT-MCM complex

The primary biochemical function of the MCM complex, specifically the MCM4/6/7 core, is unwinding of the DNA strands (Ishimi, 1997; You et al., 1999). Thus, to examine whether the identified FACT-associated MCM complexes are catalytically active, we performed DNA helicase assay. Immunoprecipitates were incubated with labeled substrate and their abilities to displace annealed oligonucleotide were assayed. We found that, as compared to the control antibody

(2B12), FACT complexes precipitated by the 10D1 antibody possessed DNA helicase activity (Figure 2A). This suggests that the FACT-MCM complexes are competent in unwinding DNA *in vitro*. Furthermore, such catalysis is an ATP-dependent process, as no such activity was detected in absence of ATP, nor in the presence of nonhydrolyzable form of ATP (Figure 2B).

To further characterize the DNA helicase activity displayed by the FACT-MCM complex, we performed additional experiments on the 10D1 immunoprecipitates. 10D1 immunoprecipitates deficient in the MCM complex (isolated from *MCM4*^{RNAi} cells, Figure 1G) lost the DNA helicase activity possessed by the intact complexes (i.e., MCM4/6/7) isolated from control or *MCM3*^{RNAi} cells (Figure 2C). This result serves as strong evidence that the helicase activity of the 10D1 immunocomplexes can be attributed primarily to the associated MCM complex, but not any non-specifically associated activities. Next, to determine whether the FACT-MCM complex undergoes cell cycle-dependent functional changes similarly to the core MCM complex, we performed DNA helicase assay on immunoprecipitates isolated from different stages. We subsequently found that, as compared to G_1/S phase, the FACT-MCM complex exhibited significantly lower helicase activity during G_2 and mitosis (Figure 2D). Taken together, we conclude that the FACT-MCM complex displays specific and significant DNA helicase activity, regulation of which coincides temporally with cell cycle progression.

FACT coexists with MCM on the chromosomal replication origin

MCM is a key component of the pre-replicative complex that has been shown indispensable during the initiation and elongation steps of DNA replication. Our observation of the interaction of FACT with MCM may thus indicate a functional link between the FACT heterodimer and DNA replication. To directly assess this possibility, we first examined whether FACT is present *in vivo* at a region of known replication origin, namely the replicator associated with human lamin B2 gene. Using ChIP assay, chromatin prepared from cells synchronized at different cell cycle stages was precipitated with the 10D1 monoclonal antibody (Figure 3A). Subsequent PCR reactions using specific sets of primers were done to assess the existence of the lamin B2 origin sequence (Figure 3A, lanes 1-6) or, as a control, sequence of a distant non-transcribed region (lanes 7-9) (see Experimental Procedures) in the immunoprecipitates. As shown in Figure 3A, at equal loads of chromatin DNA preparations, we were able to demonstrate specific occupancy of FACT in the ori region in asynchronously growing cells (compare lanes 2 and 5) and, furthermore, a modest enrichment of such binding during the G_1/S transition (compare lanes 1 and 2). Low, if any, origin association of FACT was detectable in mitotic cells (lane 3),

consistent with our observation that FACT dissociated from condensed chromatin during mitosis (Tan and Lee, 2004).

Since FACT is generally known as a transcription factor, we next aimed to analyze whether the above observation is a result of transcription-coupled recruitment. Inhibition of mRNA transcription by α-amanitin, a specific inhibitor of RNA polymerase II, did not seem to alter the binding of FACT to the lamin B2 origin, as shown by the ChIP result (Figure 3B). Additionally, we found that RNA transcript levels of the two gene loci that flank the lamin B2 origin, lamin B2 and TIMM 13, remained relatively constant during G_1/S transition. We therefore postulate that the increased association of FACT with the origin upon S-phase entry (Figure 3A, lanes 1 & 2) is independent of the transcription activity of neighboring genes. Taken together, occupancy of FACT in lamin B2 origin area may be associated primarily with DNA replication.

Despite the contact of FACT with an endogenous origin region in a chromatin context, it remains a distinct possibility that the FACT-MCM complex exists (or functions) in a non-chromatin-bound form. To address the issue of whether both MCM and FACT simultaneously assemble in this ori area, a two-step, sequential ChIP assay was performed (Figure 3D). First, sonicated chromatin fragments were immunopurified by anti-MCM4 antibodies. The specific presence of DNA fragments corresponding to lamin B2 ori in this precipitate, but not that of pre-immune sera, was confirmed by PCR (Figure 3D, lane 3 and data not shown). This result agrees with the previous observations on (the origin-binding of) MCM3 and other components of the pre-RC (Abdurashidova et al., 2003). We then used the FACT antibody to perform a second round of ChIP on chromatin recovered from the first round, and analyzed for the presence of lamin B2 origin DNA. Such chromatin fragments could be detected in the anti-SSRP1 but not the control precipitate (Figure 3D, compare lanes 1 and 2), thus demonstrating the co-existence of FACT and MCM molecules in a replication origin region on chromatin. The coexistence of FACT and MCM at chromosomal origin reflects the direct involvement of this complex in DNA replication. It is further in agreement with the above conjecture that the FACT-MCM complex is presumably chromatin-bound.

FACT promotes the DNA unwinding activity of the MCM helicase on nucleosomal template

FACT was initially isolated based on its ability to facilitate RNA polymerase passage on a nucleosomal template. We thus speculated that the involvement of FACT in the process of DNA replication might potentially be mediated by a similar mechanism wherein the chromatin unwinding (or passage) activity of MCM, through

interacting with FACT, is upregulated. To test this hypothesis, we first generated a forked, linear DNA template of ~200bp on which the unwinding activity of MCM can be assessed and mononucleosomal particles can be assembled (Figure 4A,B). As shown in Figure 4C, purified MCM2/4/6/7 complex possessed activity toward such DNA substrate (lanes 2-4 & 6), whereas purified recombinant FACT heterodimer did not (lanes 7-9). The helicase activity of MCMs was reduced considerably, however, when nucleosome was introduced onto the template, suggesting that the MCM helicase might be minimally active, or even inert, on chromatin *in vivo* (Figure 4D). Interestingly, the addition of the recombinant FACT heterodimers moderately relieved the nucleosome-dependent inhibition on the activity of MCM. Lack of nucleosomal DNA unwinding by FACT alone indicates that such DNA strand separation was specifically induced by MCM but not contaminating activities in the FACT fraction.

Next, to elucidate whether such functional cooperation between FACT and MCM depends on their physical interaction, we performed the helicase assay again with the addition of protein fragments that were shown to weaken the FACT-MCM association (Figure 1H). When the FACT-MCM complex was partially disrupted by the MCM4 deletion construct, their catalytic activity on the nucleosomal template correspondingly dropped (Figure 4D, compare lanes 5 and 7). On the other hand, the control constructs did not exhibit such effect (lanes 6 & 8). Moreover, in the presence of the MCM4 fragment, the intrinsic helicase activity of the complex on the naked DNA substrate remained unaltered (Figure 4D, lane 3). This indicates that the observed reduction of the nucleosomal DNA unwinding emanated specifically from disruption of the FACT-MCM complex. Together, these data imply a positive regulatory role of FACT on the MCM-mediated DNA unwinding during chromosomal replication.

FACT is partly associated with the endogenous DNA replication activity

Next, to further delineate the functional consequence of FACT's functional interaction with MCM, we sought to determine whether FACT is associated with the cellular DNA replication activity. To this end, we first performed co-immunoprecipitation experiments to examine potential association of FACT with other factors of the pre-replicative complex (pre-RC), which also resides on the origin. Endogenous Cdc6 was found in the FACT immunocomplexes (Figure 5A). However, we did not detect association of FACT with ORC1, as well as replicating enzymes such as DNA polymerase δ (data not shown).

Next, to directly analyze the distribution of FACT in relation to DNA replication sites, we performed confocal microscopic studies on BrdUTP-pulse labeled cells. Although uniformly localized in the nucleoplasm, FACT exhibited a partial spatial

overlap with the punctative DNA replication foci, a pattern characteristic of cells undergoing initial stages of the S phase (see cells marked with "S-early", Figure 5B). Interestingly, localization of FACT also coincided with replicating heterochromatin and perinulcear region in the late S-phase cells ("S-late", Figure 5B). These observations suggest that the FACT heterodimer may be present at replication sites throughout DNA synthesis.

The occupancy on the origin as well as physical and spatial association with DNA replication machinery may evidence a regulatory function of FACT on the initial step of DNA replication. We therefore wanted to study if the function of the origin is FACT-dependent. Using a quantitative origin mapping procedure devised by Giacca, Pelizon, and Falaschi (Giacca et al., 1997), which entails isolation of nascent DNA and quantification of specific origin DNA fragments by a competitive PCR technique (see Experimental Procedures), activity of the lamin B2 replicator can be assessed. DNA fragments (0.7-1.5 kb) were purified from the cells and subsequently subjected to competitive PCR using origin-specific (B48) and control (B13) primer sets. Based on the quantification results, the relative abundance of the B48-amplified sequences then serves as a measurement of the origin activity. As a control, knockdown of MCM4 expression by RNAi resulted in a nearly complete abolishment of origin activity (<10%) (data not shown and Figure 5C), a phenotype closely consistent with the essential role of MCM component during DNA replication initiation. In the background of down-regulated FACT, we found that the activity of lamin B2 replicator in the RNAi cells was reduced to about 30% of the control, as shown by a corresponding drop in the relative abundance of nascent DNA molecules stemmed from the activated origin (see Figure 5C, upper panel and the quantitative determination in the histogram). This result demonstrates that FACT may be needed for the optimal function of the replication origin.

Another approach to directly examine FACT's replicative function is through an *in vitro* DNA replication system. This was established by utilizing frog demembraned sperm chromatin, instead of naked DNA, as the template for appropriately monitoring replication activity in HeLa nuclear extracts (Blow and Laskey, 1986). Upon isotopic incorporation-based reaction and by gel electrophoresis of the extracted sperm DNA, we observed the labeled DNA within a discrete region on the gel (Figure 5D, lane 2), indicative of DNA synthesis and similar to the reported observations using *Xenopus* egg and *Drosophila* embryonic extracts (Blow and Laskey, 1986; Chesnokov et al., 1999). Furthermore, this activity to replicate the sperm chromatin can be attributed mainly to the DNA polymerase-associated replication machinery within the HeLa nuclear extracts, since reactions including pre-treatment of aphidocolin or sperm chromatin alone yielded undetectable signals (Figure 5D, lane 1 and data not shown).

Moreover, removal of MCM4, and consequentially other subunits of the MCM complex, from the extracts (Figure 5E, right panel) led to a similarly significant decline in the activity to replicate added sperm chromatin (Figure 5D, lane 6). Consistent with the established replicative role of MCM, this result demonstrates the essential nature of the MCM complex in the synthesis of duplex DNA. Next, as a direct test of FACT's involvement in endogenous replication activity, replication assay on FACT-depleted nuclear extracts was also performed. After two rounds of immunoprecipitation with bound 10D1 antibody, which depleted the extracts almost entirely of the heterodimers (Figure 5E, left panel), the replication activity in the extracts was reduced to about 30% of that in the mock-depleted extracts (Figure 5C, lane 3, and right panel). Partial restoration of the replication activity (~80% of the mock control) can be achieved by complementing the FACT-depleted extracts with increasing amounts of recombinant FACT (lanes 4 & 5 and right panel) or immunopurified FACT (data not shown).

Next, to address the biological significance of FACT's putative replicative function, we undertook the siRNA approach. Stable lines of HeLa cells with down-regulated SSRP1 expression were established via vector-based siRNA (see Experimental Procedures, Figure 5F). By monitoring the behaviors of the cell populations synchronously traversing S phase, we found that the *SSRP1*^{RNAi} cells moved through S phase at a slower pace and reached the G_2/M stage approximately 4 hours later than control cells. Such delayed S phase progression is consistent with the finding in yeast (Schlesinger and Formosa, 2000) and, with the above data, indicate an essential role of FACT in proper progression of DNA replication.

The replicative role of FACT is evolutionarily conserved

Labib et al. previously demonstrated that degradation of yeast MCM (yMCM) proteins in early S phase poses an irreversible block to subsequent resumption of DNA replication (Labib et al., 2000). To investigate the possibility that yeast FACT (yFACT) may share similar role in controlling DNA replication, we studied the effects of transiently inactivating Spt16 and Pob3 at early S phase. We arrested strains with conditional mutant alleles of Spt16 or Pob3 as well as the corresponding wild-types at 24°C in the early S phase before shifting to 37°C to inactivate the gene products. The cultures were then returned to 24°C for 2 more hours to allow recovery. At each stage of the experiment, viability was monitored by plating the cells at 24°C. As shown in Figure 6A, inactivation of yFACT at the G_1/S transition (after the activation of early replicative origins) resulted in a pronounced loss of viability in some of the mutant strains. Furthermore, viability of these strains was not fully restored by re-establishing permissive culture at 24°C. Hence, similar to the mutant phenotypes of the yMCMs

(Labib et al., 2000), down-regulating yFACT led to an irreversible inhibition on the resumption of stalled replication fork progression. Thus, our present results suggest that preservation of properly functioning Spt16 and Pob3 is essential for maintaining replication progression.

To further characterize the evolutionary conservation of the replicative function of FACT, we asked whether *Drosophila* FACT and MCM interacts and if FACT is functionally linked to DNA replication in the fly. To this end, we used transgenic fly line capable of expressing FLAG-tagged dSSRP or FLAG-tagged dMCM6. From the embryonic extract of the FLAG-dSSRP line, both subunits of the dFACT were immunoprecipitated by the anti-FLAG antibody (Figure 6B, left panel). Based on the specific immunoreactive signals by the anti-pan MCM antibodies, dMCMs were also present in the dFACT immunocomplexes. Conversely, ectopically expressed FLAG-dMCM6, which existed as part of the endogenous dMCM complex (Schwed et al., 2002), also specifically associated with the dFACT heterodimer in the embryos of the transgenic flies (the UFM strain, right panel of Figure 6B). Together, these immunochemical results demonstrate that a *Drosophila* counterpart of the human FACT-MCM protein complexes also exists.

To directly examine the role of dFACT in DNA replication, we undertook both biochemical and genetic approaches. First, we compared the DNA synthesis activity of mock-treated *Drosophila* embryonic extracts and those immunodepleted of dFACT (Figure 6C, upper two panels). Similar to what was observed with the human FACT (Figure 5D), chromosomal DNA replication was noticeably reduced upon removal of dFACT (Figure 6C, bottom panel), demonstrating its importance in optimal DNA synthesis. Next, we used a mutant fly strain in which a mutation of the *dre4* gene (homologue of the human Spt16) renders the gene product functional in a temperature-sensitive manner (Radyuk et al., 2000; Sliter and Gilbert, 1992). We first subjected embryos (6-8 hrs) of this strain as well as those of the wild-type control to BrdU treatment and subsequently detected analog incorporation using anti-BrdU antibody. Under permissive rearing temperature (25°C), hundreds of cells were stained positively for BrdU in a single embryo of either phenotype (Figure 6D and data not shown). When the temperature was shifted to 30°C, BrdU incorporation in the mutant was reduced (Figure 6D, bottom two panels), whereas wild-type embryos exhibited normal pattern of replicating cells (top panel). These results thus indicate that such severe defects in DNA replication and cell proliferation may be an underlying cause of the early lethality (1st to 2nd instar larval stage) of the *dre4* mutant strain (Radyuk et al., 2000), and strongly suggest a conservation of the replicative role of FACT across eukaryotic species.

Discussion

In the present study, we identified the MCM complexes as novel interacting proteins of the FACT heterodimer, and performed functional characterization of this interaction. The catalytic activity of FACT-MCM complexes is regulated in a cell cycle-dependent manner that temporally correlates its activity with S phase. In addition to its association with the replicative helicase complex, the involvement of FACT in DNA replication was further strengthened by its co-existence with MCM on the replication origin as well as its functional association with the endogenous replication activity. Finally, we demonstrated that a potential mechanism of FACT's replicative function lies in facilitating the nucleosomal DNA helicase activity of the MCM complex. Taken together, these results directly implicate the highly conserved role of FACT in the progression of DNA replication and further outline a model of the collaborative function of the FACT and MCM complexes in chromatin unwinding (Figure 7).

Chromatin is inhibitory in nature to various DNA transactions, generally by rendering the DNA template structurally inaccessible. Despite extensive studies on dissecting the modular organization and temporal regulation of DNA replication, the role of chromatin in this process has not been fully addressed. Based on our observation, nucleosomes impose a structural hindrance that efficiently reduces the DNA helicase activity of MCM (Figure 4C), an effect similarly observed in the case of RNA polII-mediated transcription (Orphanides et al., 1998). Our identification of FACT as a replication factor clearly signifies the importance of chromatin structure in modulating progression of replication and, more importantly, an intrinsic requirement of a chromatin remodeling/loosening mechanism. Indeed, putative involvement of chromatin modifiers, such as CHRAC, HBO1, Sir2p, and Rpd3, in DNA replication was recently identified (Aggarwal and Calvi, 2004; Alexiadis et al., 1998; Burke et al., 2001; Pappas et al., 2004). New findings linking histone hyperacetylation to active origins lend further support to the notion that DNA replication is under epigenetic control (Aggarwal and Calvi, 2004; Stedman et al., 2004). Taken together, these observations emphasize the direct role of chromatin context in DNA replication, and suggest that, as in transcription, multiple factors/complexes, coordinately or independently, may constitute the chromatin regulatory mechanism during replication events (Figure 7).

Existence of replication-associated chromatin-modulating factors other than FACT is further evident in our results. Down-regulation of FACT led to considerable, but not complete, loss of replication origin function (Figure 5B) and chromatin replication activity (Figure 5C), suggesting the partially redundant nature of FACT's

activity. Moreover, results from the *in vitro* helicase assay indicate that, even in the presence of FACT, the nucleosomal duplex unwinding by MCM could not be fully restored to a level comparable to that on the naked DNA template (Figure 4C). We thus speculate that the establishment of an optimal nucleosomal structure in which the template is readily accessible to MCM cannot be achieved by FACT alone but requires the concerted action of different activities (histone modification, for instance). Together, these observations point to a regulatory function of FACT's activity, as well as possible involvement of other factors, in facilitating chromatin replication.

Although we were able to detect amplified origin DNA fragments in the FACT immunoprecipitates (Figure 3A), the exact binding site on the sonicated fragments (average size of 500-600 bp) is not yet known. The genomic region that contains the replication start site within the lamin B2 replicon has been extensively characterized. The initiation site is encompassed in an *in vivo*-protected area (the origin-protected area, OPR), on which certain proteins of the pre-RC have been known to occupy (Abdurashidova et al., 2003; Paixao et al., 2004). Additionally, the *in vivo* footprinting analysis indicates that the extension of OPR, although fluctuates, usually remains around 100 nucleotides. These characteristics imply that the core region of the lamin B2 replicon is relatively free of nucleosomes (assembly of which should predictably lead to a footprint protection of around 150 bp) and therefore FACT as well. Thus, association of FACT with this region may be a result of binding to potentially nucleosomal regions flanking the origin rather than to the core region (OPR) directly. Furthermore, based on the observation of the modest enrichment of FACT on the origin at the G_1/S stage (Figure 3A, lane 2), it is likely that, as accompanied by the recruitment of FACT, the local chromatin structure around the origin undergoes replication-associated changes. Taken together, our results spatially link FACT to replication origin and provide additional evidence of the importance of nucleosomal structure on regulating origin firing and replication progression.

From our immunoprecipitation experiments we identified the existence of complexes formed between FACT and MCM2/4/6/7 (Figure 1). Based on the previous observations on the stable formation of different subassemblies among the six MCM subunits (Lee and Hurwitz, 2000; Schwacha and Bell, 2001; Tye and Sawyer, 2000; You et al., 1999), we postulate that such assembly may presumably be "catalytic". Indeed, we subsequently detected DNA unwinding activities in this immunocomplex. However, association of MCM3, MCM5, or the "regulatory" MCM2/3/5 subcomplex with the FACT heterodimer was not detected in the present study but cannot be excluded.

The cell cycle-dependent manner through which FACT and MCM functionally interact with each other was demonstrated by the immunocomplex helicase assay

(Figure 2C). The observed behaviors of the FACT-associated MCM4 recall the mitotic-specific hyperphosphorylation and functional down-regulation of MCM4, as reported previously (Ishimi and Komamura-Kohno, 2001). Such mode of regulation, presumably through a conserved mechanism, suggests the involvement of cell cycle regulators such as Cdk2/cyclin A or cyclin B (Fujita et al., 1998; Hendrickson et al., 1996; Ishimi and Komamura-Kohno, 2001; Pereverzeva et al., 2000). In addition to catalytic inactivation, mitotic hyperphosphorylation of MCM4 may concomitantly lead to dissociation from chromatin, as indicated by these reports. Additionally, in accordance with the finding by Ishimi and Komamura-Kohno (Ishimi and Komamura-Kohno, 2001), we observed a moderate but reproducible increase in catalytic activity of the FACT-MCM complex isolated from the G_1/S-synchronized cells as compared to those at other phases (Figure 2C). Despite a greater extent of mobility shift of MCM4 in the S phase immunocomplex (compare lanes 1 and 2, Figure 2B), it is unclear at present whether or which signaling pathway underlies such modification and catalytic activation. Cdc7/Dbf4 (DDK) complex is a likely candidate kinase regulator (Masai and Arai, 2002). Identification of these regulators may be a future research subject, and understanding of this signaling pathway will aid in further characterization of FACT-MCM or MCM proteins in general. Together, the functional consequences of these phosphorylation events reflect the critical integration of replication with cell cycle as well as a temporal resetting of MCM activity.

Experimental Procedures

Preparation of recombinant proteins and MCM complex

FLAG-hSpt16p and His_6-SSRP1 were expressed by baculovirus-infected insect cells (Sf9) and purified by anti-FLAG (M2) immunoaffinity column and Ni-NTA agarose (Qiagen), respectively, according to the manufacturer's instructions and procedures described previously (Tan and Lee, 2004). For the *in vitro* DNA replication (Figure 5D) and chromatin unwinding (Figure 4) assays, the expression and purification of recombinant FACT heterodimer were done according to the procedures outlined elsewhere (Belotserkovskaya et al., 2003). Purification of the MCM2/4/6/7 complex was done based on a previously established protocol (Ishimi, 1997). pGEX plasmids encoding GST-MCMs are generous gifts from Dr Hiroshi Nojima. Bacterial expression of these proteins and purification by the Glutathione Sepharose 4B (Amersham Pharmasia) were based on manufacturer's protocols.

Antibodies and Western blot analysis

Generation of monoclonal antibodies against SSRP1 (2B12/control and 10D1) and

hSpt16p was described previously (Tan and Lee, 2004). Polyclonal antibodies against human pan-MCM and DNA pol δ catalytic chain monoclonal antibody (A-9) was respectively purchased from BD biosciences and Santa Cruz Biotechnology. Monoclonal antibody against Cdc6 and rabbit antisera against MCM3, MCM4, MCM5, and MCM6 were produced with the following peptide antigens and affinity purified by Dagene (Taiwan). Cdc6: QLTIKSPSKREL; MCM3: SDTEEEMPQVHTPKTAD; MCM4: SRRGRATPAQTPRSED; MCM5: KEVADEVTRPRPSGE; MCM6: KYLQLAEELIRPERNT. Polyclonal antibody against MCM2 was generated using a recombinant protein fragment of MCM2 (a.a. 792-892). Western blot analysis was performed after electrophoretic separation of polypeptides by 7.5% or 10% SDS-PAGE and trasfer to Hybond-C membranes. Blots were probed with the indicated primary and appropriate secondary antibodies, and detected by ECL chemiluminescence (Amersham).

Immunoprecipitation, immunodepletion, and in vitro pull-down assay

HeLa cells were extracted using a buffer containing: 20 mM HEPES (pH 7.4), 0.2 M NaCl, 0.5% TX100, 5% glycerol, 1 mM EDTA, 1 mM EGTA, 10 mM β-glycerophosphate, 2 mM Na_3VO_4, 1 mM NaF, 1 mM DTT, plus protease inhibitors. For preparation of nuclear extracts, HeLa nuclei were isolated and lysed in nuclear extraction buffer (10 mM HEPES with pH 7.9, 10 mM KCl, 0.1 mM EDTA, 0.1 mM EGTA, 0.1% TX-100, 0.4 M NaCl, 10% glycerol and protease inhibitors). All immunoprecipitations were done with the indicated antibodies prebound to protein G-Sepharose (Amersham), and washed in the cell lysis buffer. Similar conditions were applied to the immunodepletion experiment. Nuclear extracts were subjected to incubation with protein G-Sepharose beads conjugated with control or the indicated specific antibodies. After pelleting the beads, the supernatants were subjected to a second round of immunoprecipiation. The resultant supernatant extracts were subsequently frozen in aliquots before being used in DNA replication assay. For the *in vitro* pull-down assay, purified and bound GST-MCMs were independently incubated with eluted FLAG-hSpt16p or His_6-SSRP1 in the cell lysis buffer. Protein-bound beads were then washed four times in the same buffer.

Please include the plasmid for disruption of MCM4-FACT interaction.

Gel-filtration fractionation

Gel filtration chromatography was done using a precalibrated Sephacryl S-400 HR column with a bed volume of 135 ml (Pharmacia). Nuclear lysate preparation, chromatographic settings, and fraction collection and processing were done essentially as reported previously (Tan and Lee, 2004).

Plasmid-based dsRNAi

To establish a plasmid-based dsRNAi system targeting endogenous SSRP1, annealed oligonucleotides corresponding to partial SSRP1 sequence were designed and ligated to the pSuper.neo+GFP (OligoEngine) according to the manufacturer's instructions. The cDNA sequence of the targeted SSRP1 mRNA region is: 5'-TGGCAAGACCTTTGACTAC-3' (nucleotides 677-695). The same sequence in the inverted orientation was used as the non-specific dsRNAi control. (You have to include sequences for MCM4 and MCM3 RNAi.)

Cell culture, transfection, and cell cycle analysis

All HeLa cells were maintained in Dulbecco's modified Eagle's medium supplemented with 10% fetal bovine serum and 100 units/ml penicillin and streptomycin. Cells were transfected using Lipofectamine (GIBCO) according to the manufacturer's instructions. Generation of cell lines stably harboring dsRNAi was done by first transfection of the pSuper plasmid and subsequent clone selection in the presence of 1 mg/ml G418. Protein expression knockdown was confirmed by Western blot using anti-SSRP1 mAb. For monitoring S phase progression (Figure 5E), collection of HeLa cells at different stages of the cell cycle was achieved by the double thymidine block method, as outlined previously (Tan and Lee, 2004). Procedure for the FACS analysis was also described in the same report. α-Amanitin (Sigma) was dissolved in phosphate-buffered saline (PBS). Treatment of drug (of the indicated concentrations) was performed for 12-14 hr in a 37°C cell culture incubator.

DNA helicase assay

The substrate for the helicase assay was a partially heteroduplex DNA containing a 17-mer oligonuleotide (5'-GTTTTCCCAGTCACGAC-3') annealed to the M13mp18 (+) circular ssDNA (Amersham). Before annealing, the oligonuleotide was labeled at the 5' end with [γ-^{32}P]ATP by polynucleotide kinase. The annealed substrate was subsequently purified on the MicroSpin G50 column (Amersham). MCM-containing FACT immunocomplexes were isolated by the indicated antibodies and from HeLa cells at the specified cell cycle stages. With the exception of the immobilized source of enzymatic activities, DNA helicase assay was performed essentially as described previously (You et al., 2003), with the addition of approximately 10-20 fmol of substrate. After deproteination, samples were resolved by electrophoresis (15% native PAGE/TBE) and autoradiographed.

Yeast strains and media

Yeast strains are generated and generously provided by Dr. Tim Formosa (Formosa et al., 2001; Schlesinger and Formosa, 2000). All strains harbor the indicated Spt16 or Pob3 (wild-type or temperature-sensitive mutants) plasmids to complement the deleted genome locus. Strains were grown in the rich medium YP (1% yeast extract, Difco, plus 2% bacto peptone, Difco) supplemented with glucose to a final concentration of 2%.

S phase-associated yeast viability assay

Yeast viability assay was done based on the previous work on yMCM (Labib et al., 2000). Yeast cells were grown to 10^7 cells per ml in YPG (YP+glucose). Cell cycle was blocked at G_1-S phase by adding HU (hydroxyurea), as a powder, to a final concentration of 0.2 M. After growing at 24°C for two generation times, which lasted about 4 hr, growth was shifted to 37°C for 3 hr to inactivate the mutant proteins. The cultures were then returned to 24°C for two more hours for recovery. Samples were taken throughout the experiment at specified time points. Cell viability was determined by plating cells on YPG plates (2% agar) and counting the number of colonies after three days of incubation at 24°C.

Fly stocks and BrdU labeling

The temperature-sensitive *dSpt16/dre4* mutant fly (*ru dre4*^{e55} *st*) and the control (*ru dre4*$^{+}$ *st e*^{s}) were generously provided by W. C. Orr (Radyuk et al., 2000). The FLAG-dSSRP-expressing fly strain harbors the *P[w*$^{+}$*, hsp83>FLAG-dSSRP]* element. The FLAG-dMCM6 (*P[w*$^{+mc}$*, Ub>FLAG-dMCM6]*) transgenic line was established and kindly provided by B. Calvi (Schwed et al., 2002). For examination of DNA replication, embryos (6-8 hr) were reared at 25°C or 30°C at egg-laying. They were subsequently collected and processed for BrdU labeling/immunostaining essentially as described in a standard protocol (Shermoen, 2000), with the exceptions of BrdU concentration (30 μg/ml), labeling length (15 min), and length of acid treatment (60 min). The anti-BrdU monoclonal antibody was purchased from Becton-Dickinson Biosciences (1:100). Secondary antibody incubation was done for 2 h using Alexa 488 conjugated goat anti-mouse IgG (Moleular Probes, Inc). Stained embryos were analyzed with the Zeiss LSM 510 Meta confocal laser-scanning microscope, using a 20X objective lens. For detection of DNA replication sites in HeLa cells, cells on coverslips were pulse labeled with 10 μM BrdU at 37°C for 30 min. Upon fixation and permeabilization, cells were subjected sequentially to acid treatment and trypsin enzymetic digestion before being stained. Stained cells were analyzed using a 100X oil immersion objective lens.

Chromatin immunoprecipitation

Chromatin immunoprecipitation assays were modified from previously described methods (Su et al., 2003). Briefly, HeLa cells (exponentially growing or synchronized) were cross-linked with 1% formaldehyde for 10 min at 37 °C. The nuclei were isolated and sonicated into oligonucleosomes of ~500-600 bp in length. The sheared chromatin was immunoprecipitated overnight with protein G-agarose previously bound with the 10D1 or control antibody. After extensive washes, the immunoprecipitates were subjected to deproteination and cross-linking reversal. For the sequential ChIP experiment, precipitate from the first round (anti-MCM4 IP) was recovered by an elution solution (1% SDS and 0.1 M $NaHCO_3$) and used to perform a second round of ChIP using the 10D1 or control antibody. The presence of genomic DNA in the precipitates was detected by PCR with the B48 primer set and a background primer set. The background primers anneal to a region with no annotated genes, 30 kb upstream of the lamine B2 origin sequence on chromosome 19, and have the following sequences: 5'-CTATGCCAAGCCCATTCTAGGTCCT-3' (sense); 5'-GCAGGGAAACTGTGCACAGCAAGAG-3' (antisense).

Upon amplification for 27-30 cycles, the products were resolved by 2% agarose gels and visualized with ethidium bromide staining.

RT-PCR

First-strand cDNA synthesis was done with the SuperScript II Reverse Transcriptase (Invitrogen). Sequences of the primers used to PCR-amplify the lamin B2, TIMM 13, or GADPH transcripts are as follows. lamin B2: 5'-TGCAGGAGGAGCTGGACTTC-3' (sense); 5'- CTTCCGGAACTTGTCCCGCT-3' (antisense). TIMM 13: 5'-GACAAGTGTTTCCGGAAGTG -3' (sense); 5'-TATGAGGCTGACTTGGGCAC -3' (antisense). GADPH: 5'-ACCACAGTCCATGCCATCAT-3' (sense); 5'-TCCACCACCCTGTTGCTGTA-3' (antisense).

Competitive PCR-based measurement of origin activity

Genomic DNA was isolated from 5 × 10^7 exponentially growing HeLa (control or dsRNAi) cells based on the protocol described elsewhere (Paixao et al., 2004). Upon fractionation by sucrose gradient centrifugation, single-stranded (nascent) DNA fragments of the length 0.7 to 1.5 kb were isolated and concentrated by ethanol precipitation. Competitive PCR analysis was performed with the B48 and B13 primer sets (Dx/Sx), sequences of which were detailed in the above publication. To generate a competitor template, a DNA segment that carries the tandem sequences of the B48

and B13 primers at two ends separated by a 180-bp linker DNA sequence in middle was amplified by PCR. Thus, as the result of competitive PCR, the length of competitor products would be ~240 bp, as opposed to 160 bp of the genomic DNA products. Competitive PCR amplification was done with a constant volume of nascent DNA and decreasing amounts of the competitor fragment, at the conditions of 95℃ for 30 s, 56℃ for 25 s, and 72℃ for 25 s (40 cycles). PCR products were resolved on agarose gel (2%) and stained with ethidium bromide. Intensities of DNA bands on the UV-illuminated images were quantitatively determined by a Fujifilm Luminescent Image Analyzer LAS-1000plus and the software Image Gauge. To determine the amount of target genomic molecules in the nascent DNA sample, linear relationship between the competitor/target genomic DNA (C/T) ratios and the concentrations of the input competitor was first plotted and deduced. Based on the equation, the target DNA concentration was then calculated as the amount of competitor DNA at C/T = 1. For each type of cell line, the ratio of the DNA products amplified by B48 and B13 primer pairs was subsequently evaluated. The capacity of the endogenous origin in promoting DNA replication initiation was then compared between control and SSRP1-knockdown cells.

In vitro DNA replication reactions

Demembranated frog sperm nuclei were prepared using the method described previously (Blow and Laskey, 1986). Nuclei, at the final concentration of 5000 sperm nuclei/μl, were stored in the SuNaSp/glycerol buffer (250 mM sucrose, 75 mM NaCl, 0.5 mM spermidine, 0.15 mM spermine, and 30% glycerol) at -70℃. Conditions for the *in vitro* replication reaction were based on a modification of a previous study (Okuhara et al., 1999). Immunodepleted HeLa nuclear extracts or *Drosophila* embryo extracts were mixed with 50 mM phosphocreatine (Sigma), 100 μg/ml creatine phosphokinase (Sigma), and 10 μCi/ml of [α-^{32}P]dCTP (Amersham). Sperm nuclei were added at a final concentration of 100 nuclei/μl and incubation was performed at 30℃ for 1 hr. The reaction was stopped by addition of 0.5% SDS, 20 mM EDTA, and 50 μg proteinase K (final concentration). Upon incubation at 37℃ for 1 hr, DNA was then extracted from the mixture with phenol/chloroform, ethanol precipitated, and finally analyzed by electrophoresis in agarose gel (0.8 %) and autoradiography. In some of the experiments, the immunodepleted extracts were, as indicated, supplemented with aphidocolin (10 μg/ml) or purified recombinant FACT.

Chromatin unwinding assay

A PCR-based strategy was applied to generate the linear, tailed DNA substrate for the nucleosome reconstitution and the helicase assay (Figure 6A). The template backbone

is a 180 bp-long sequence covering part of the mouse AGP gene promoter (Chang et al., 1990). Two sets of primer pairs were designed to generate from PCR amplification two types of DNA segments, "upper" and "lower". The sequences of the primers are: 5'-TTTTTTTTTTTTTTCGGCAGGAGTCTGTGTCA-3' ("upper" forward); 5'-GTTTGGATGGTGCAGC-3' ("upper" reverse); 5'-AAAAAAAAAAAAAACGGCAGGAGTCTGTGTCA-3' ("lower" forward); 5'-GGGGGGGTTTGGATGGTGCAGC-3' ("lower" reverse). Both PCR products were purified and mixed equally and then subjected to denaturing (95℃ for 5 min) and renaturing (65℃ for 15 min, 37℃ for 1 hr). Only one of the four likely renatured intermediates (25% of the final products) can subsequently be isotopically labeled by T4 DNA polymerase in the presece of [α-^{32}P]dCTP. Nucleosome cores were prepared from HeLa cells (Mizzen et al., 1999) and reconstituted onto the 200-bp, end-labeled DNA fragment by octamer transfer method (Studitsky et al., 1995; Utley et al., 1996). Helicase assay was performed on the naked DNA or nucleosomal templates with the indicated amounts of factors and proceeded with the conditions as described above. The reactions were terminated and deproteinated by the addition of EDTA (20 mM), SDS (1%), and 5 μg of proteinase K. Degree of unwinding was observed as in the DNA helicase assay (7.5% native PAGE/TBE).

Acknowledgements

We thank Tim Formosa for the yeast strains; Hiroshi Nojima for the MCM plasmids; William C. Orr and Brian Calvi for the fly strains. We are especially grateful to Drs. Ruey-Hwa Chen, Ching-Jin Chang, and Margaret S. Ho for critical reading of the manuscript, and members of the S.C. Lee and C.T. Chien labs for technical assistance. This work was supported by National Science Council Grants NSC93-2320-B002-105 and the Institute of Biological Chemistry, Academia Sinica (to S.C.L.), and National Health Research Institute (NHRI) postdoctoral fellowship award PD9302 (to B.C.T.).

Reference

Abdurashidova, G., Danailov, M. B., Ochem, A., Triolo, G., Djeliova, V., Radulescu, S., Vindigni, A., Riva, S., and Falaschi, A. (2003). Localization of proteins bound to a replication origin of human DNA along the cell cycle. EMBO J *22*, 4294-4303.

Aggarwal, B. D., and Calvi, B. R. (2004). Chromatin regulates origin activity in Drosophila follicle cells. Nature *430*, 372-376.

Alexiadis, V., Varga-Weisz, P. D., Bonte, E., Becker, P. B., and Gruss, C. (1998). In vitro chromatin remodelling by chromatin accessibility complex (CHRAC) at the SV40 origin of DNA replication. EMBO J *17*, 3428-3438.

Aparicio, O. M., Weinstein, D. M., and Bell, S. P. (1997). Components and dynamics

of DNA replication complexes in S. cerevisiae: redistribution of MCM proteins and Cdc45p during S phase. Cell *91*, 59-69.
Bell, S. P., and Dutta, A. (2002). DNA replication in eukaryotic cells. Annu Rev Biochem *71*, 333-374.
Belotserkovskaya, R., Oh, S., Bondarenko, V. A., Orphanides, G., Studitsky, V. M., and Reinberg, D. (2003). FACT facilitates transcription-dependent nucleosome alteration. Science *301*, 1090-1093.
Blow, J. J., and Laskey, R. A. (1986). Initiation of DNA replication in nuclei and purified DNA by a cell-free extract of Xenopus eggs. Cell *47*, 577-587.
Burke, T. W., Cook, J. G., Asano, M., and Nevins, J. R. (2001). Replication factors MCM2 and ORC1 interact with the histone acetyltransferase HBO1. J Biol Chem *276*, 15397-15408.
Chang, C. J., Chen, T. T., Lei, H. Y., Chen, D. S., and Lee, S. C. (1990). Molecular cloning of a transcription factor, AGP/EBP, that belongs to members of the C/EBP family. Mol Cell Biol *10*, 6642-6653.
Chesnokov, I., Gossen, M., Remus, D., and Botchan, M. (1999). Assembly of functionally active Drosophila origin recognition complex from recombinant proteins. Genes Dev *13*, 1289-1296.
Davey, M. J., Indiani, C., and O'Donnell, M. (2003). Reconstitution of the Mcm2-7p heterohexamer, subunit arrangement, and ATP site architecture. J Biol Chem *278*, 4491-4499.
Formosa, T., Eriksson, P., Wittmeyer, J., Ginn, J., Yu, Y., and Stillman, D. J. (2001). Spt16-Pob3 and the HMG protein Nhp6 combine to form the nucleosome-binding factor SPN. EMBO J *20*, 3506-3517.
Fujita, M., Yamada, C., Tsurumi, T., Hanaoka, F., Matsuzawa, K., and Inagaki, M. (1998). Cell Cycle- and Chromatin Binding State-dependent Phosphorylation of Human MCM Heterohexameric Complexes. A ROLE FOR cdc2 KINASE. J Biol Chem *273*, 17095-17101.
Giacca, M., Pelizon, C., and Falaschi, A. (1997). Mapping replication origins by quantifying relative abundance of nascent DNA strands using competitive polymerase chain reaction. Methods *13*, 301-312.
Gilbert, D. M., Miyazawa, H., and DePamphilis, M. L. (1995). Site-specific initiation of DNA replication in Xenopus egg extract requires nuclear structure. Mol Cell Biol *15*, 2942-2954.
Gillespie, P. J., and Blow, J. J. (2000). Nucleoplasmin-mediated chromatin remodelling is required for Xenopus sperm nuclei to become licensed for DNA replication. Nucleic Acids Res *28*, 472-480.
Hendrickson, M., Madine, M., Dalton, S., and Gautier, J. (1996). Phosphorylation of

MCM4 by cdc2 protein kinase inhibits the activity of the minichromosome maintenance complex. Proc Natl Acad Sci U S A *93*, 12223-12228.
Hyrien, O., Maric, C., and Lucas, I. (1997). Role of nuclear architecture in the initiation of eukaryotic DNA replication. Biochimie *79*, 541-548.
Hyrien, O., Maric, C., and Mechali, M. (1995). Transition in specification of embryonic metazoan DNA replication origins. Science *270*, 994-997.
Iizuka, M., and Stillman, B. (1999). Histone acetyltransferase HBO1 interacts with the ORC1 subunit of the human initiator protein. J Biol Chem *274*, 23027-23034.
Ishimi, Y. (1997). A DNA helicase activity is associated with an MCM4, -6, and -7 protein complex. J Biol Chem *272*, 24508-24513.
Ishimi, Y., and Komamura-Kohno, Y. (2001). Phosphorylation of Mcm4 at specific sites by cyclin-dependent kinase leads to loss of Mcm4,6,7 helicase activity. J Biol Chem *276*, 34428-34433.
Keller, D. M., and Lu, H. (2002). p53 serine 392 phosphorylation increases after UV through induction of the assembly of the CK2.hSPT16.SSRP1 complex. J Biol Chem *277*, 50206-50213.
Keller, D. M., Zeng, X., Wang, Y., Zhang, Q. H., Kapoor, M., Shu, H., Goodman, R., Lozano, G., Zhao, Y., and Lu, H. (2001). A DNA damage-induced p53 serine 392 kinase complex contains CK2, hSpt16, and SSRP1. Mol Cell *7*, 283-292.
Kelly, T. J., and Brown, G. W. (2000). Regulation of chromosome replication. Annu Rev Biochem *69*, 829-880.
Labib, K., Tercero, J. A., and Diffley, J. F. (2000). Uninterrupted MCM2-7 function required for DNA replication fork progression. Science *288*, 1643-1647.
Lee, J. K., and Hurwitz, J. (2000). Isolation and characterization of various complexes of the minichromosome maintenance proteins of Schizosaccharomyces pombe. J Biol Chem *275*, 18871-18878.
Lee, J. K., and Hurwitz, J. (2001). Processive DNA helicase activity of the minichromosome maintenance proteins 4, 6, and 7 complex requires forked DNA structures. Proc Natl Acad Sci U S A *98*, 54-59.
LeRoy, G., Orphanides, G., Lane, W. S., and Reinberg, D. (1998). Requirement of RSF and FACT for transcription of chromatin templates in vitro. Science *282*, 1900-1904.
Masai, H., and Arai, K. (2002). Cdc7 kinase complex: a key regulator in the initiation of DNA replication. J Cell Physiol *190*, 287-296.
Mizzen, C. A., Brownell, J. E., Cook, R. G., and Allis, C. D. (1999). Histone acetyltransferases: preparation of substrates and assay procedures. Methods Enzymol *304*, 675-696.
Okuhara, K., Ohta, K., Seo, H., Shioda, M., Yamada, T., Tanaka, Y., Dohmae, N.,

Seyama, Y., Shibata, T., and Murofushi, H. (1999). A DNA unwinding factor involved in DNA replication in cell-free extracts of Xenopus eggs. Curr Biol *9*, 341-350.
Orphanides, G., LeRoy, G., Chang, C. H., Luse, D. S., and Reinberg, D. (1998). FACT, a factor that facilitates transcript elongation through nucleosomes. Cell *92*, 105-116.
Orphanides, G., Wu, W. H., Lane, W. S., Hampsey, M., and Reinberg, D. (1999). The chromatin-specific transcription elongation factor FACT comprises human SPT16 and SSRP1 proteins. Nature *400*, 284-288.
Paixao, S., Colaluca, I. N., Cubells, M., Peverali, F. A., Destro, A., Giadrossi, S., Giacca, M., Falaschi, A., Riva, S., and Biamonti, G. (2004). Modular structure of the human lamin B2 replicator. Mol Cell Biol *24*, 2958-2967.
Pappas, D. L., Jr., Frisch, R., and Weinreich, M. (2004). The NAD(+)-dependent Sir2p histone deacetylase is a negative regulator of chromosomal DNA replication. Genes Dev *18*, 769-781.
Pereverzeva, I., Whitmire, E., Khan, B., and Coue, M. (2000). Distinct Phosphoisoforms of the Xenopus Mcm4 Protein Regulate the Function of the Mcm Complex. Mol Cell Biol *20*, 3667-3676.
Radyuk, S. N., Klichko, V. I., and Orr, W. C. (2000). Catalase expression in Drosophila melanogaster is responsive to ecdysone and exhibits both transcriptional and post-transcriptional regulation. Arch Insect Biochem Physiol *45*, 79-93.
Schlesinger, M. B., and Formosa, T. (2000). POB3 is required for both transcription and replication in the yeast Saccharomyces cerevisiae. Genetics *155*, 1593-1606.
Schwacha, A., and Bell, S. P. (2001). Interactions between two catalytically distinct MCM subgroups are essential for coordinated ATP hydrolysis and DNA replication. Mol Cell *8*, 1093-1104.
Schwed, G., May, N., Pechersky, Y., and Calvi, B. R. (2002). Drosophila minichromosome maintenance 6 is required for chorion gene amplification and genomic replication. Mol Biol Cell *13*, 607-620.
Shermoen, A. W. (2000). BrdU Labeling of Chromosomes. In *Drosophila* Protocols, W. Sullivan, Ashburner, M., Hawley, R.S., ed. (Cold Spring Harbor, NY, Cold Spring Harbor Laboratory Press), pp. 57-65.
Simpson, R. T. (1990). Nucleosome positioning can affect the function of a cis-acting DNA element in vivo. Nature *343*, 387-389.
Sliter, T. J., and Gilbert, L. I. (1992). Developmental arrest and ecdysteroid deficiency resulting from mutations at the dre4 locus of Drosophila. Genetics *130*, 555-568.
Stedman, W., Deng, Z., Lu, F., and Lieberman, P. M. (2004). ORC, MCM, and Histone Hyperacetylation at the Kaposi's Sarcoma-Associated Herpesvirus Latent Replication Origin. J Virol *78*, 12566-12575.
Studitsky, V. M., Clark, D. J., and Felsenfeld, G. (1995). Overcoming a nucleosomal

barrier to transcription. Cell *83*, 19-27.
Su, W. C., Chou, H. Y., Chang, C. J., Lee, Y. M., Chen, W. H., Huang, K. H., Lee, M. Y., and Lee, S. C. (2003). Differential activation of a C/EBP beta isoform by a novel redox switch may confer the lipopolysaccharide-inducible expression of interleukin-6 gene. J Biol Chem *278*, 51150-51158.
Tan, B. C., and Lee, S. C. (2004). Nek9, a novel FACT-associated protein, modulates interphase progression. J Biol Chem *279*, 9321-9330. Epub 2003 Dec 9302.
Tanaka, T., Knapp, D., and Nasmyth, K. (1997). Loading of an Mcm protein onto DNA replication origins is regulated by Cdc6p and CDKs. Cell *90*, 649-660.
Tye, B. K., and Sawyer, S. (2000). The hexameric eukaryotic MCM helicase: building symmetry from nonidentical parts. J Biol Chem *275*, 34833-34836.
Utley, R. T., Owen-Hughes, T. A., Juan, L. J., Cote, J., Adams, C. C., and Workman, J. L. (1996). In vitro analysis of transcription factor binding to nucleosomes and nucleosome disruption/displacement. Methods Enzymol *274*, 276-291.
Wittmeyer, J., and Formosa, T. (1997). The Saccharomyces cerevisiae DNA polymerase alpha catalytic subunit interacts with Cdc68/Spt16 and with Pob3, a protein similar to an HMG1-like protein. Mol Cell Biol *17*, 4178-4190.
Wittmeyer, J., Joss, L., and Formosa, T. (1999). Spt16 and Pob3 of Saccharomyces cerevisiae form an essential, abundant heterodimer that is nuclear, chromatin-associated, and copurifies with DNA polymerase alpha. Biochemistry *38*, 8961-8971.
You, Z., Ishimi, Y., Mizuno, T., Sugasawa, K., Hanaoka, F., and Masai, H. (2003). Thymine-rich single-stranded DNA activates Mcm4/6/7 helicase on Y-fork and bubble-like substrates. EMBO J *22*, 6148-6160.
You, Z., Komamura, Y., and Ishimi, Y. (1999). Biochemical analysis of the intrinsic Mcm4-Mcm6-mcm7 DNA helicase activity. Mol Cell Biol *19*, 8003-8015.

Figure Legends

Figure 1

Replicative helicase MCM is a novel interacting protein of FACT.

(A) FACT-associated complexes were immunoprecipitated from HeLa nuclear extracts using αSSRP1 mAb 10D1, resolved by and shown on a silver-stained gel (also see Tan and Lee, 2004). Specific SSRP1-interacting protein bands around 100 kD that are absent in the control immunoprecipitates (not shown) were identified by mass spectrometry as MCM4 and MCM6. The 120-kD band represents a previously identified associated protein, Nek9 (Tan and Lee, 2004).

(B) Western blot analysis of HeLa whole cell extracts, as well as the different

immunocomplexes targeted by control (2B12) and αSSRP1 (10D1) mAbs. Immunoblotting was done using the indicated antibodies against pan-MCM or individual subunits. The positions of MCM2, MCM4/6, and MCM7 in the IP are indicated by the black, gray, and white arrowheads, respectively. The amount of the Input is equivalent to 1/40 the IP. The identity of the protein band, marked by the asterisk, is unknown.

(C) Western blot analysis of HeLa cell extracts and different immunoprecipitates targeted by pre-immune serum (PI), αMCM3, and αMCM4 antibodies. Immunoblotting was done using the specified antibodies (shown on the right side of each panel). The amount of the Input is equivalent to 1/40 of the IP.

(D) HeLa nuclear extracts were subjected to gel filtration chromatography using Sephacryl S-400. Fraction numbers as well as size markers are denoted on the bottom. Fractions were probed with the specified antibodies. Selected fractions were further subjected to immunoprecipitation using 10D1 and subsequently probed with the indicated antibodies (bottom three panels).

(E) MCM heterotetramer (MCM2/4/6/7, left panel) and recombinant FACT heterodimer (FLAG-hSpt16/ His_6-SSRP1, right panel) were isolated as described in Materials and Methods and visualized by silver-stained gel. *In vitro* pull-down assay was done using the anti-FLAG M2 agarose, with the indicated combinations of protein complexes. Presence of specifically bound proteins was detected by the indicated antisera (bottom panel).

(F) Bacterially expressed GST and GST-fused MCMs were used as baits in the *in vitro* pull-down assay. Presence and purity of the immobilized proteins were seen on Coomassie blue-stained gels. Presence of bound FLAG-hSpt16 or His_6-SSRP1 protein was detected by immunoblotting with M2 or αSSRP1 antibodies, respectively. The diagram shown below the panels depicts the presence or absence of interaction between specific deletion constructs of MCM4 and the FACT subunits.

(G) Ablation of endogenous MCM3 and MCM4 expression was achieved by RNAi. Equal loadings of whole cell extracts ("Input") derived from HeLa cells transiently harboring control-, MCM3-, or MCM4-targeting dsRNA were resolved by SDS-PAGE and blotted with the indicated antibodies. Lysates (30x of Input) were immunoprecipitated with 10D1 (bottom three panels, "IP: 10D1") and subsequently probed with the indicated antibodies.

(H) *In vitro* pull-down assay was done as in (E). GST (lane 2) or GST-fused deletion constructs of MCM3 and MCM4 (GST-$MCM4_{1-100}$, lane 3; GST-$MCM3_{1-100}$, lane 4) was added to the binding mixture. Precipitated rFACT as well as co-precipitated MCMs were probed with the indicated antibodies.

Figure 2

The FACT-MCM complex is regulated in a cell cycle-dependent manner.

(A) Immunocomplexes were isolated as in Figure 1B and subjected to DNA helicase assay. The reaction was conducted on a radiolabeled, 17-mer oligonucelotide annealed on the M13 single-stranded DNA ("HD", heteroduplex DNA). Upon protein removal, reaction mixtures were resolved by native gel. The locations of the annealed and displaced substrates (ssDNA) on the gel are shown. Displacement of the annealed substrate by heat denaturation is also shown (Boiled).

(B) The DNA helicase activity of the FACT-MCM complex is ATP-dependent. The displacement of 17-mer oligonucleotide (SS) from the heteroduplex substrate (HD) by the 10D1-immunocomplex was assayed in the presence (lane 2) or absence (lane 3) of ATP, or in the presence of ATP-γS (lane 4).

(C) HeLa cell extracts were prepared from control (lanes 2 & 3), *MCM4*^{RNAi} (lane 4), or *MCM3*^{RNAi} (lane 5) cells as in Figure 1F. The displacement activity of the mock- (lane 2) or 10D1- (lanes 3-5) immunocomplex isolated from these extracts is shown.

(D) FACT-associated immunocomplex was isolated by mAb 10D1 from HeLa cells at different cell cycle stages: exponentially growing (lane 1), G_1/S phase (lane 2), S phase at 1 hr after double-thymidine block (lane 3), S phase at 3 hr (lane 4), and M phase (lane 5) and G_2 (lane 6). The immunoprecipitate was subsequently subjected to DNA helicase assay as above.

Figure 3

FACT coexists with MCM on the chromosomal replication origin.

(A) ChIP was performed as described in Experimental Procedures. Sonicated chromatin fragments were prepared from cells at different stages: asynchronous (lanes 1, 4, & 7), G_1/S (lanes 2, 5, & 8), and G_2/M (lanes 3, 6, & 9). Immunoprecipitation was done with either control (lanes 4-6) or 10D1 (lanes 1-3, 7-9) antibody. Products from final PCR analysis using primers specific to lamin B2 origin (lanes 1-6) or to a non-transcribed region (lanes 7-9) were resolved by 1.5% agarose gel.

(B) HeLa cells were treated with various concentrations of α-amanitin to inhibit RNA polII-transcription. Binding of FACT to the lamin B2 origin under such treatment was monitored by the ChIP assay using the 10D1 antibody, as in (A).

(C) The mRNA level of the lamin B2 and TIMM3 genes in asynchrous or double thymidine-arrested (G_1/S) HeLa cells were examined by RT-PCR. Expression level of GAPDH was used as a loading control.

(D) Coexistence of FACT and MCM on origin was demonstrated by a sequential ChIP experiment. Chromatin was first immunoprecipitated by MCM4 antibody (lane 3). A second round of ChIP was performed using control (lane 1) or 10D1 (lane 2) antibody

and the precipitate recovered from the first round of ChIP. The presence of DNA fragments corresponding to the lamin B2 origin in the second ChIP was assessed by PCR.

Figure 4

FACT promotes the DNA unwinding activity of the MCM helicase on nucleosomal template.

(A) Schematic representation of the strategy for generating a liner, tailed DNA template by PCR. The presence of 5' dT (15-mer) tail is known to increase the helicase activity of MCM (You et al., 2003). Asterisk marks the site of labeling. See Experimental Procedures for details.

(B) Reconstitution of nucleosome cores onto the ~200-bp, end-labeled DNA fragment. Aliquot of the transfer reactions were analyzed and bands corresponding to reconstituted nucleosomes and free DNA are indicated.

(C) Helicase assay was performed with the indicated amounts of isolated MCM2/4/6/7 (lanes 2-4, 6) or purified recombinant FACT (lanes 7-9). Reactions were done on the free DNA substrate. Deprotienated reaction products were resolved by native gel electrophoresis. M, 100 bp ladder DNA marker. Denaturation of the DNA substrate by heat is also shown ("Boiled", lane 5).

(D) DNA helicase assay was carried out as in (C), except with the use the reconstituted nucleosomal template. Unwinding of the nucleosomal DNA by various combinations of the MCMs and/or FACT complexes (amounts indicated on top) were monitored by autoradiography.

(E) DNA helicase activity of the FACT-MCMs complex (FACT:MCMs = 1 μg:0.2 μg) was assayed on the naked DNA (lanes 1-4) or the nucleosomal (lanes 5-8) template, as described above. Before reaction, the complexes were pre-incubated with buffer (lanes 1 & 5), GST (lanes 2 & 6), or GST-fused deletion constructs of MCM3 and MCM4 (GST-MCM4$_{1\text{-}100}$, lanes 3 & 7; GST-MCM3$_{1\text{-}100}$, lanes 4 & 8).

In (C), (D), and (E): the positions of the double- and single-stranded fragments are indicated by arrowheads and arrows, respectively.

Figure 5

FACT is partly associated with the endogenous DNA replication activity.

(A) HeLa WCE was subjected to immunoprecipitation with a control (2B12) or 10D1 antibody. The extract input was served as a control for the IP (1/40). Existence of pre-RC component Cdc6 in these immunoprecipitates was detected by a specific antibody.

(B) Nuclear distribution and partial co-localization of endogenous FACT and DNA

replication sites. HeLa cells were pulse-labeled with BrdU and double-stained for SSRP1 (top panels) and BrdU (middle panels). Individual and merged images (bottom panels) were generated by laser scanning confocal microscope. Cells in different stages of S-phase are marked.

(C) Competitive PCR analysis of nascent DNA molecules isolated from control, *SSRP1*^{RNAi}, and *MCM4*^{RNAi} cells (see Experimental Procedures). The dilutions of the competitor are indicated on top of the panel. M, DNA size marker. Results from amplification with the B48 primer set are shown. The positions and sizes of the amplified competitor and origin fragments are shown on the sides of the image (C and ori, 240 and 160 bp, respectively). Right panel, quantitative representation of the origin activity in the three cell types, with the activity in the control cells represented as 1. Data are averaged ± standard deviations of three independent experiments.

(D) Effect of immunodepletion on DNA synthesis was examined using sperm chromatin as a template (see Experimental Procedures). Left panel, DNA replication of sperm chromatin in aphidocolin-treated (lane 1), mock-treated (lane 2), FACT-depleted (lanes 3-5), or MCM-depleted (lane 6) extracts was measured by incorporation of α-[^{32}P] dCTP. Labeled products were subjected to eletrophoresis and autoradiography. Experiments using FACT-depleted extracts with add-back of 0.15 μg (lane 4) and 0.3 μg (lane 5) of recombinant FACT are also shown. Right panel, histogram of the DNA synthesis activity in the mock-depleted (white bar), FACT-depleted (gray) and FACT-reconstituted (dark gray) extracts, with the activity in the control extracts represented as 1. Data are averaged ± standard deviations of three independent experiments.

(E) HeLa nuclear extracts were subjected to two rounds of IP with 10D1 (left) or αMCM4 (right) antibody to respectively deplete endogenous pools of FACT or MCM. Presence of FACT or MCM in the control or depleted extracts was probed with the indicated antibodies.

(F) Ablation of endogenous SSRP1 expression was achieved by RNAi. Equal loadings of whole cell extracts derived from HeLa cells stably harboring control- or SSRP1-targeting dsRNA were resolved by SDS-PAGE and blotted with αSSRP1 and α-tubulin antibodies, as indicated (left panel). Control and *SSRP1*^{RNAi} cells were synchronized at the G_1/S junction by double thymidine block. At the indicated time points after the release, cells were harvested and subjected to DNA content analysis by FACS (right panel). Three different clones of *SSRP1*^{RNAi} cells, all with similar behaviors, were isolated and characterized. Representative data from one clone is shown.

Figure 6

The essential role of FACT in S phase progression is conserved.

(A) Yeast cell viability assay was done to monitor the effect of yFACT conditional alleles on the progression of S phase (see Experimental Procedures). Cell viability was determined by plating cells on YPG plates and counting the number of colonies after three days of incubation at 24°C. Degree of cell viability for each strain is expressed as a percentage to the colony number of the initial sample point.

(B) Identification of the FACT-MCM complex in *Drosophila*. Extracts of FLAG-dSSRP-expressing embryos were subjected to immunoprecipitation with anti-FLAG (M2) antibody or anti-HA antibody as a control (left panel). Similar immunoprecipiations were also done on the extracts of embryos with the FLAG-MCM6-expressing transgene (UFM) (right panel). Detection of tagged as well as coprecipitated proteins was achieved with Western blot analysis using the αFLAG (M2), αdSpt16, αdSSRP, and anti-pan MCM antibodies, as indicated. The amount of the Input is equivalent to 1/80 of the IP.

(C) *Drosophila* FACT heterodimer was immunodepleted from embryonic extracts using anti-dSSRP antisera. Depletion of endogenous dFACT was monitored by immunoblotting using the indicated antibodies (upper two panels). DNA replication of sperm chromatin in the mock- or depleted-embryo extracts was assayed as in Figure 5E.

(D) Embryonic cells undergoing S phase were revealed by BrdU labeling in stage 11 embryos collected from wild-type flies (at 30°C, upper), and a conditional mutant *dre4*^{e55} strain at 25°C (second panel from the top) or 30°C (in the bottom two panels, two examples of BrdU labeling in mutant embryo at restrictive temperature are shown).

Figure 7

A model that depicts the concerted action of chromatin remodeling and DNA helicase activities during replication progression.

In this model, the transition from origin binding of pre-RC (replication initiation) to origin unwinding and strand elongation is negatively regulated by chromatin structure (denoted by dark blue nucleosomes). Many of the known accessory protein factors, as well as the detailed mechanisms, that are essential for this transition are omitted for simplification of the model illustration. To overcome such inhibitory effect of nucleosomes, eukaryotic cells are equipped with different chromatin-modifying enzymes that aid in establishing a context (denoted by light blue nucleosomes) more favorable for replication progression (see Discussion). As described in this report, the human FACT is functionally linked to DNA replication through its association with

the replicative helicase MCM. By altering nucleosomal structure, FACT facilitates DNA unwinding by MCM, and potentially the accompanying strand elongation by the polymerase. Based on existing evidence, it is not yet known whether FACT and MCM functionally interact during later phase of DNA replication (marked by "?").

Figure 1

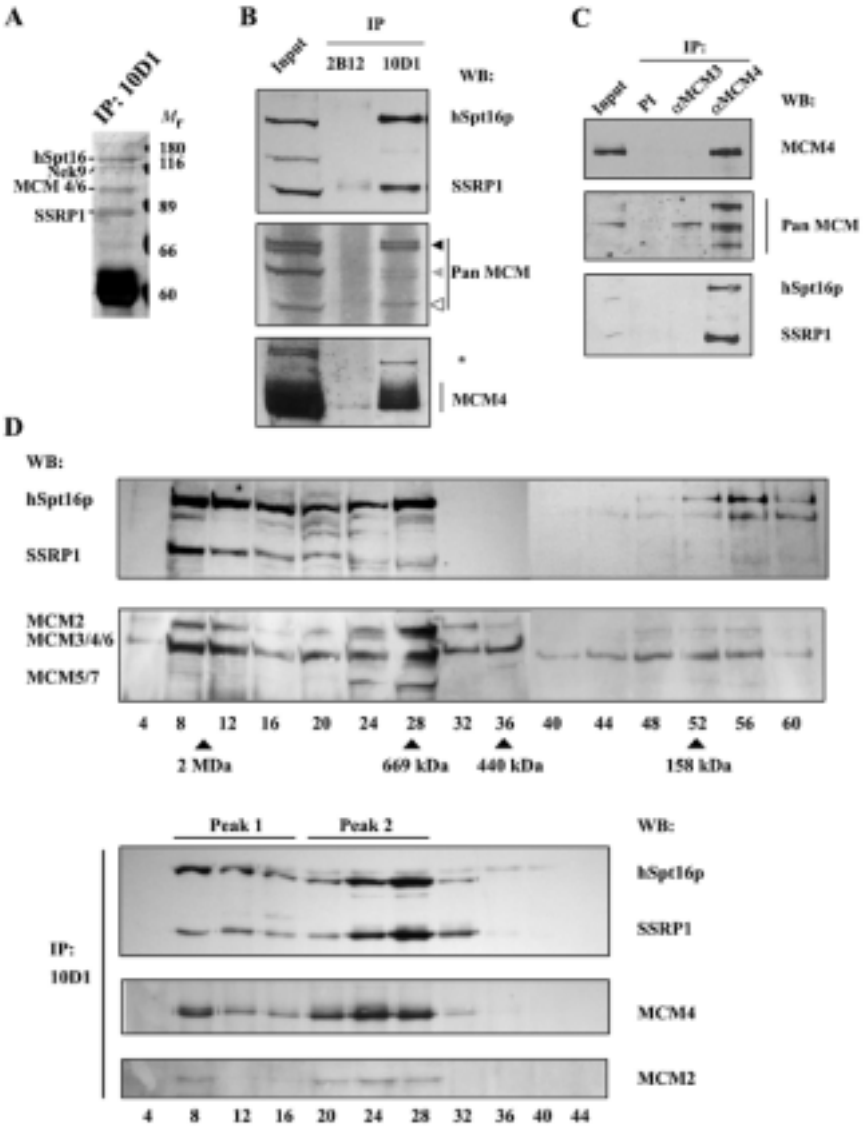
A
IP: 10D1
M_r
180
116
89
66
60
hSpt16
Nek9
MCM 4/6
SSRP1
B
IP
Input
2B12
10D1
WB:
hSpt16p
SSRP1
Pan MCM
*
MCM4
C
IP:
Input
PI
αMCM3
αMCM4
WB:
MCM4
Pan MCM
hSpt16p
SSRP1
D
WB:
hSpt16p
SSRP1
MCM2
MCM3/4/6
MCM5/7
4 8 12 16 20 24 28 32 36 40 44 48 52 56 60
2 MDa
669 kDa
440 kDa
158 kDa
Peak 1
Peak 2
WB:
hSpt16p
SSRP1
IP:
10D1
MCM4
MCM2
4 8 12 16 20 24 28 32 36 40 44

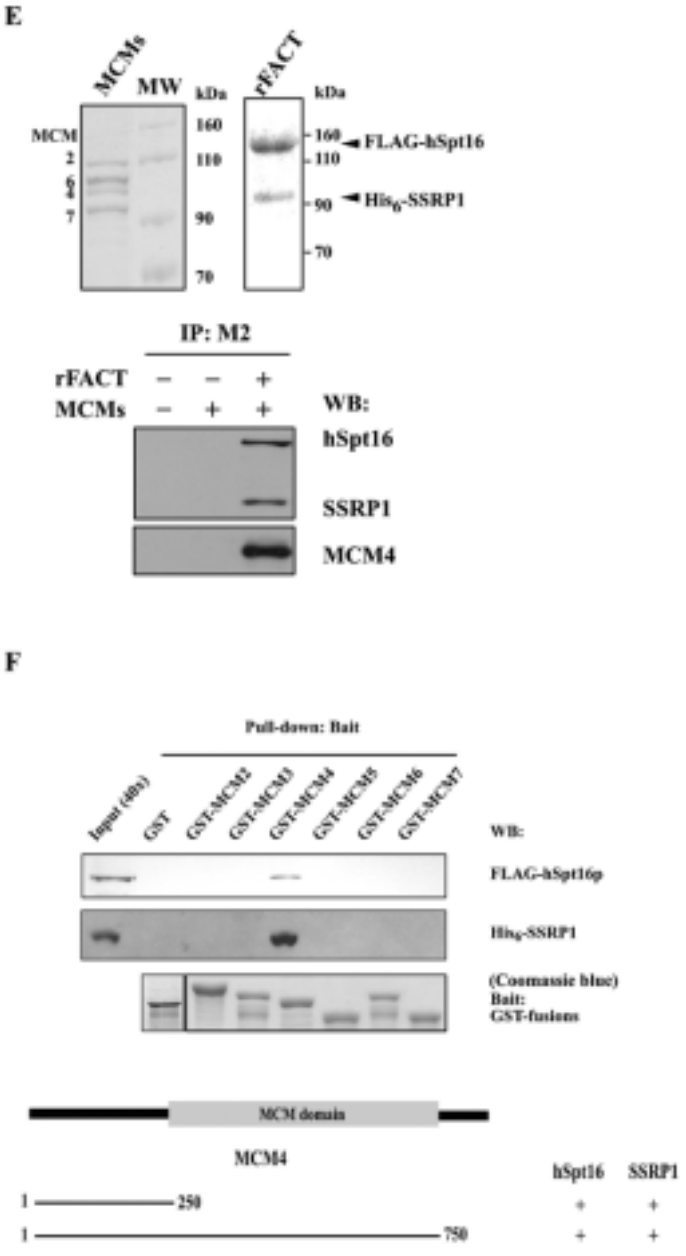
E
MCMs
MW
kDa
160
110
90
70
MCM
2
6
4
7
rFACT
kDa
160
110
90
70
FLAG-hSpt16
His6-SSRP1
IP: M2
rFACT − − +
MCMs − + +
WB:
hSpt16
SSRP1
MCM4
F
Pull-down: Bait
Input (40%)
GST
GST-MCM2
GST-MCM3
GST-MCM4
GST-MCM5
GST-MCM6
GST-MCM7
WB:
FLAG-hSpt16p
His6-SSRP1
(Coomassie blue)
Bait:
GST-fusions
MCM domain
MCM4
hSpt16
SSRP1
1 250 + +
1 750 + +
250 Stop − +
250 560 − −
560 Stop − +

Figure 2

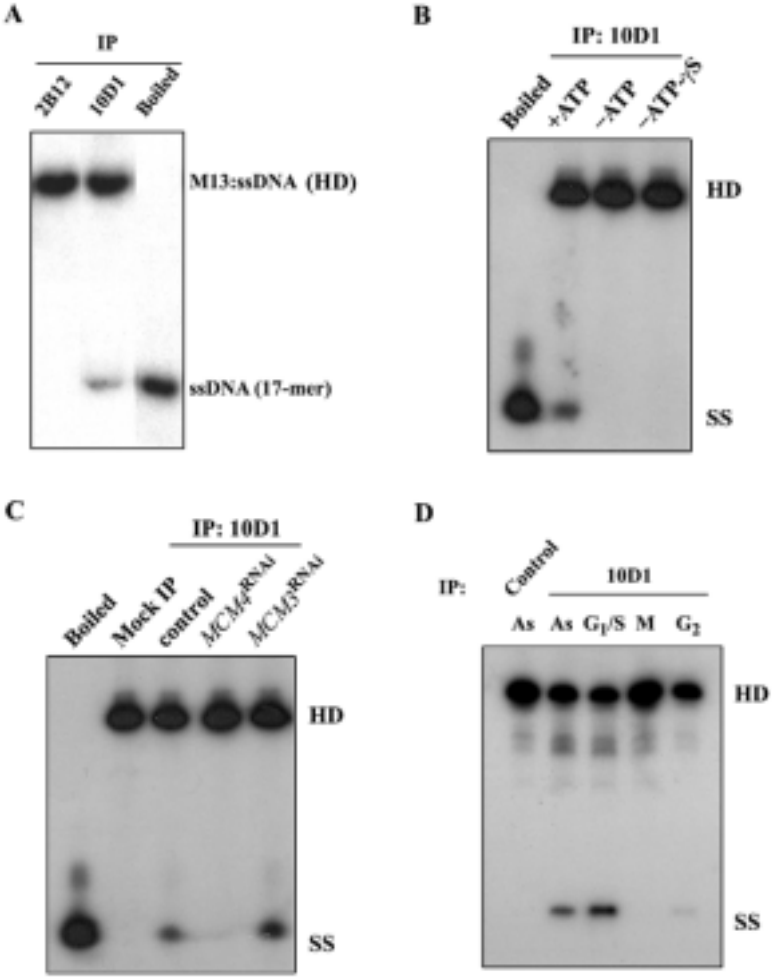
A
IP
2B12
10D1
Boiled
M13:ssDNA (HD)
ssDNA (17-mer)
B
IP: 10D1
Boiled
+ATP
−ATP
−ATP-γS
HD
SS
C
IP: 10D1
Boiled
Mock IP
control
MCM4RNAi
MCM3RNAi
HD
SS
D
IP:
Control
10D1
As
As
G1/S
M
G2
HD
SS

Figure 3

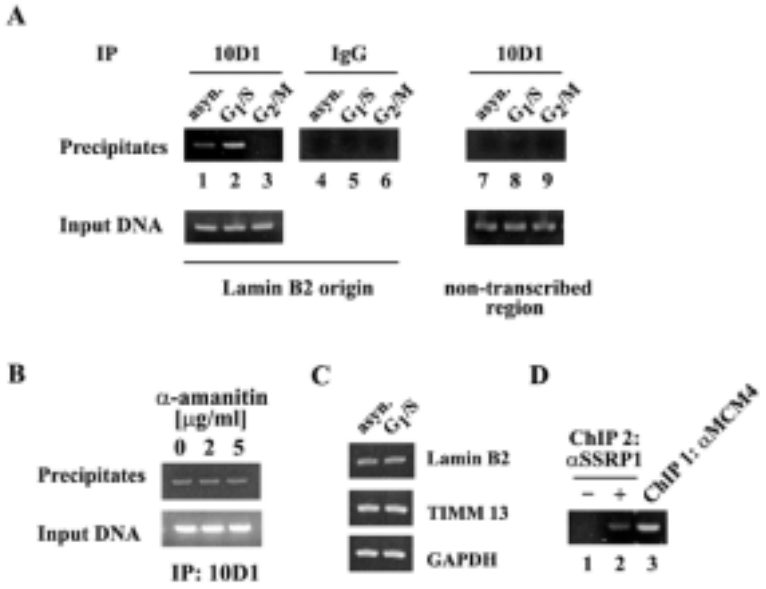
A
IP
10D1
IgG
10D1
asyn.
G1/S
G2/M
Precipitates
1 2 3 4 5 6 7 8 9
Input DNA
Lamin B2 origin
non-transcribed region
B
α-amanitin [μg/ml]
0 2 5
Precipitates
Input DNA
IP: 10D1
C
asyn.
G1/S
Lamin B2
TIMM 13
GAPDH
D
ChIP 2: αSSRP1
– +
ChIP 1: αMCM4
1 2 3

Figure 4

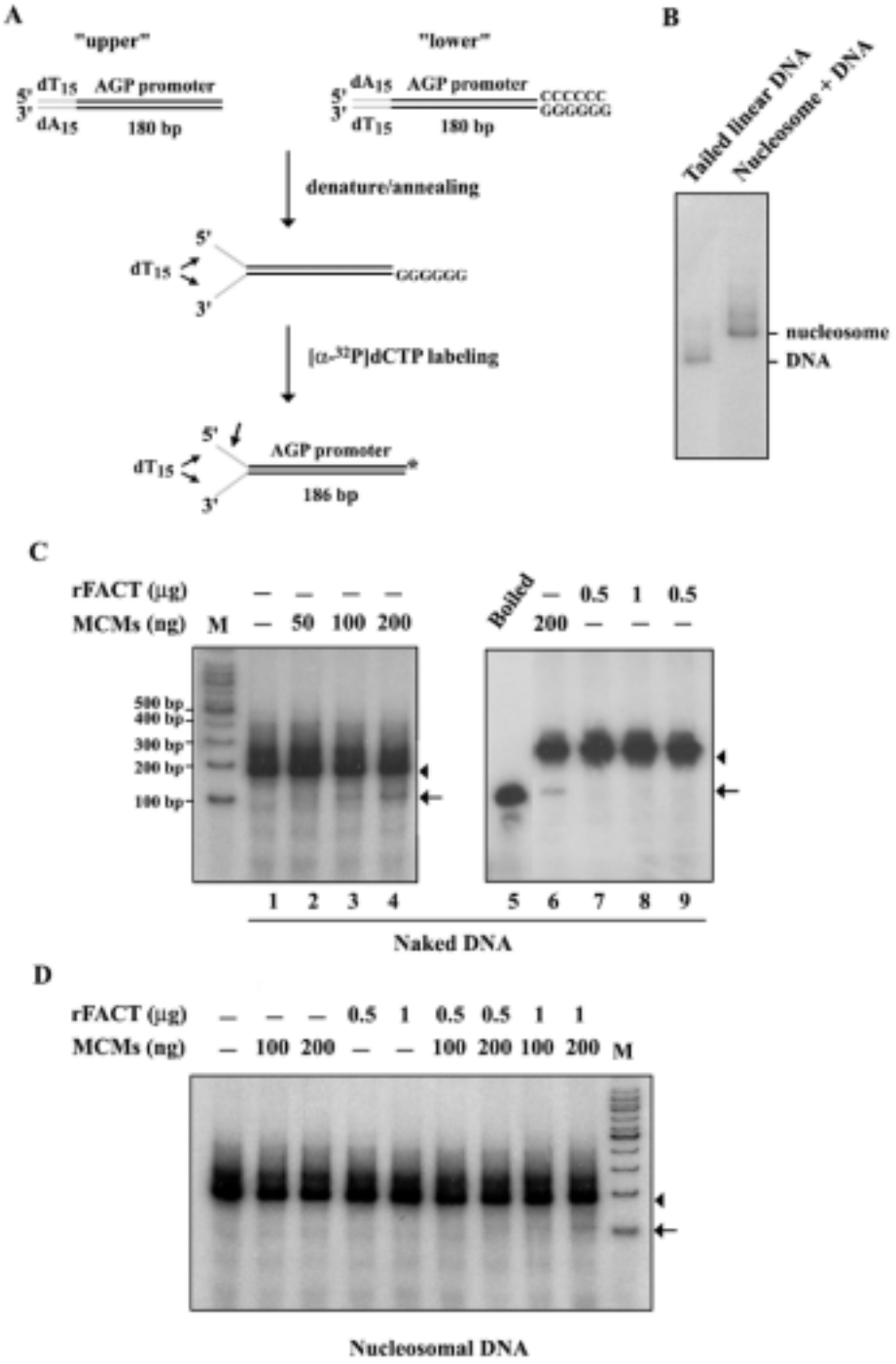
A
"upper"
"lower"
5' dT15 AGP promoter
3' dA15 180 bp
5' dA15 AGP promoter CCCCCC
3' dT15 180 bp GGGGGG
denature/annealing
5'
dT15
GGGGGG
3'
[α-32P]dCTP labeling
5'
AGP promoter
dT15
3'
186 bp
B
Tailed linear DNA
Nucleosome + DNA
nucleosome
DNA
C
rFACT (μg) — — — —
MCMs (ng) M — 50 100 200
Boiled — 0.5 1 0.5
200 — — —
500 bp
400 bp
300 bp
200 bp
100 bp
1 2 3 4
5 6 7 8 9
Naked DNA
D
rFACT (μg) — — — 0.5 1 0.5 0.5 1 1
MCMs (ng) — 100 200 — — 100 200 100 200 M
Nucleosomal DNA

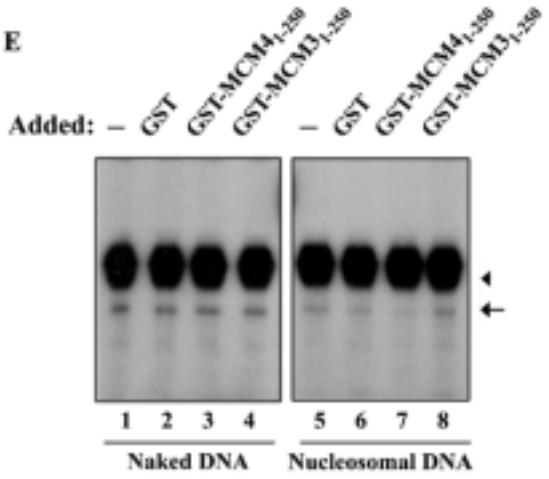
E
Added: – GST GST-MCM4 1-259 GST-MCM3 1-259 – GST GST-MCM4 1-259 GST-MCM3 1-259
1 2 3 4 5 6 7 8
Naked DNA
Nucleosomal DNA

Figure 5

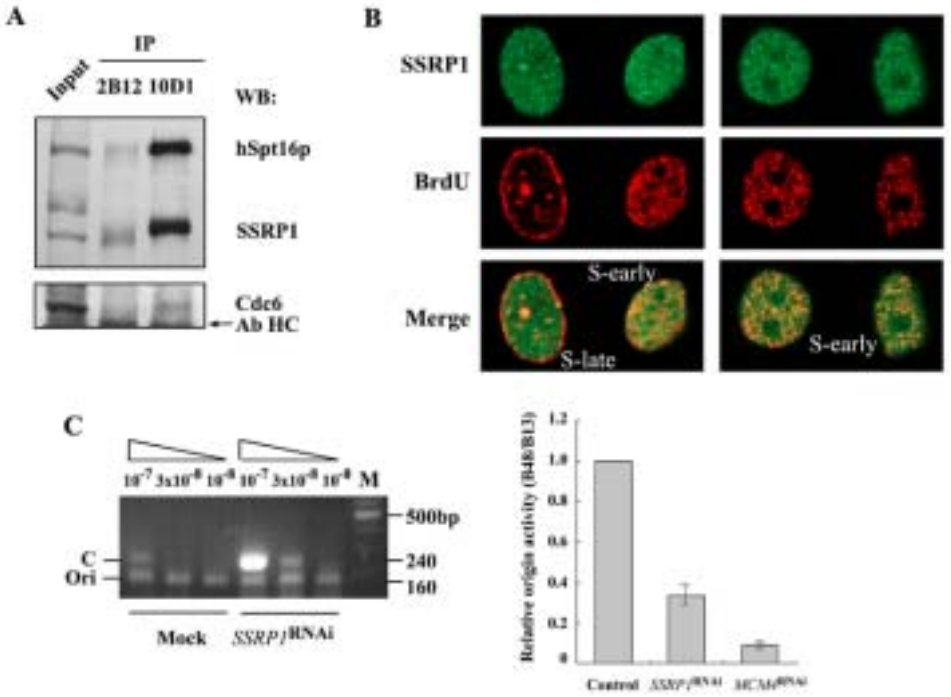
A
IP
Input
2B12 10D1
WB:
hSpt16p
SSRP1
Cdc6
Ab HC
B
SSRP1
BrdU
Merge
S-early
S-late
S-early
C
10-7 3x10-8 10-8 10-7 3x10-8 10-8 M
500bp
240
160
C
Ori
Mock
SSRP1RNAi
Relative origin activity (B48/B13)
1.2
1.0
0.8
0.6
0.4
0.2
0
Control

Figure 5

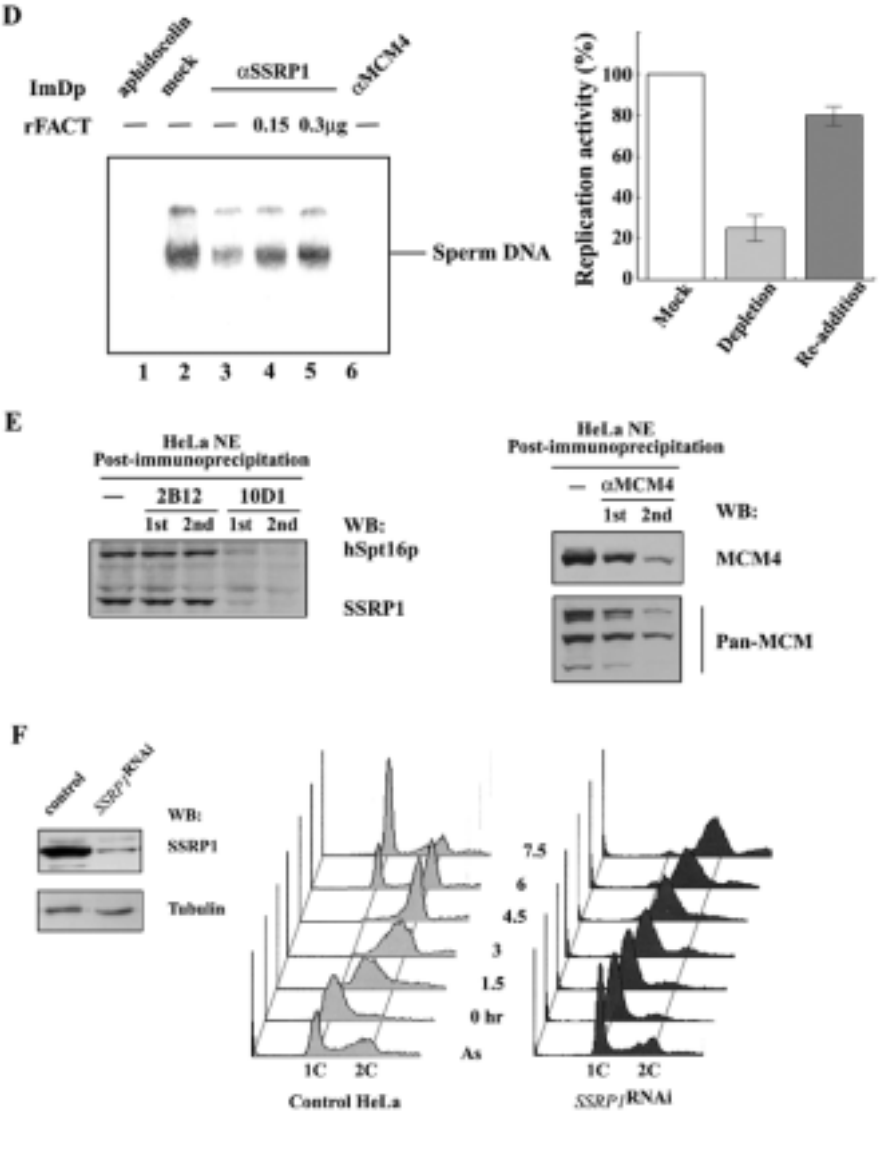
D
ImDp
aphidicolin
mock
αSSRP1
αMCM4
rFACT
0.15 0.3μg
Sperm DNA
1 2 3 4 5 6
Replication activity (%)
100
80
60
40
20
0
Mock
Depletion
Re-addition
E
HeLa NE
Post-immunoprecipitation
2B12
10D1
1st 2nd 1st 2nd
WB:
hSpt16p
SSRP1
HeLa NE
Post-immunoprecipitation
αMCM4
1st 2nd
WB:
MCM4
Pan-MCM
F
control
SSRP1RNAi
WB:
SSRP1
Tubulin
7.5
6
4.5
3
1.5
0 hr
As
1C 2C
Control HeLa
1C 2C
SSRP1RNAi

Figure 6

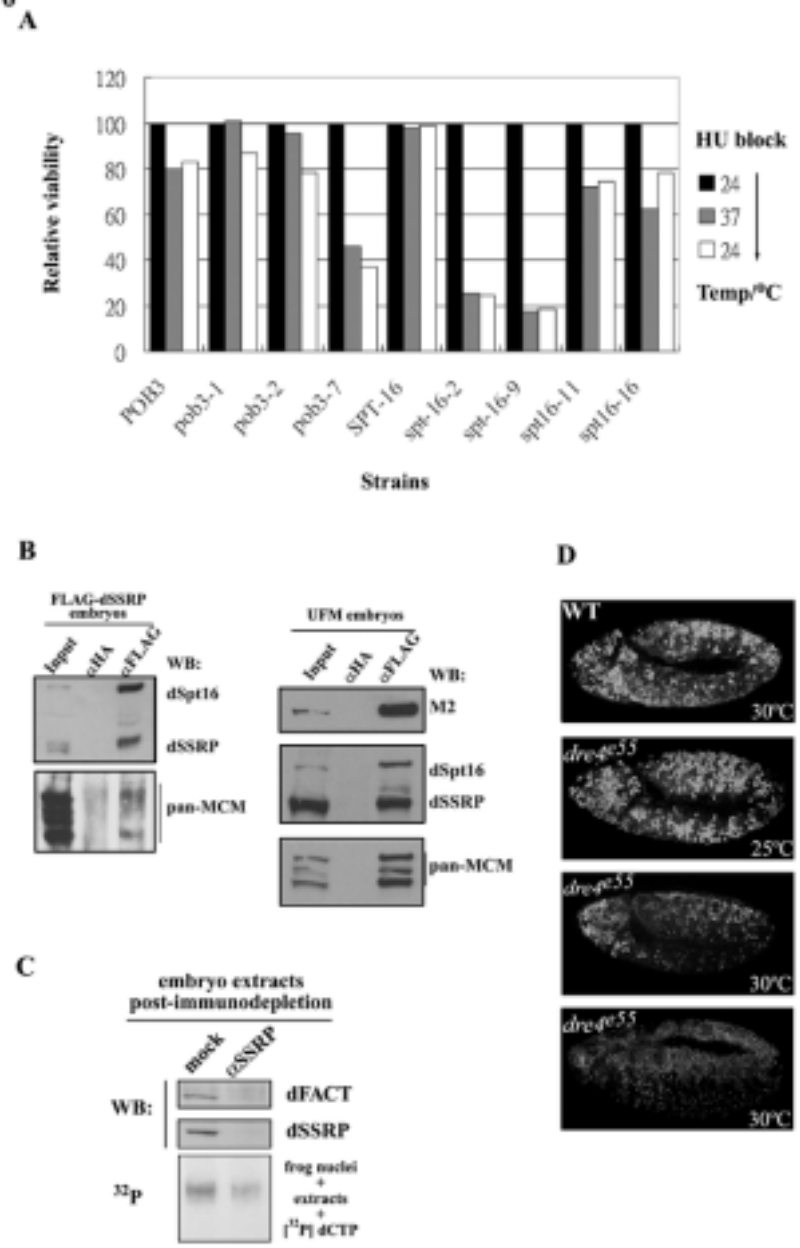
A
Relative viability
120
100
80
60
40
20
0
HU block
24
37
24
Temp/°C
POB3
pob3-1
pob3-2
pob3-7
SPT-16
spt-16-2
spt-16-9
spt16-11
spt16-16
Strains
B
FLAG-dSSRP embryos
Input
αHA
αFLAG
WB:
dSpt16
dSSRP
pan-MCM
UFM embryos
Input
αHA
αFLAG
WB:
M2
dSpt16
dSSRP
pan-MCM
C
embryo extracts post-immunodepletion
mock
αSSRP
WB:
dFACT
dSSRP
32P
frog nuclei + extracts + [32P] dCTP
D
WT
30°C
dre4e55
25°C
dre4e55
30°C
dre4e55
30°C

Figure 7

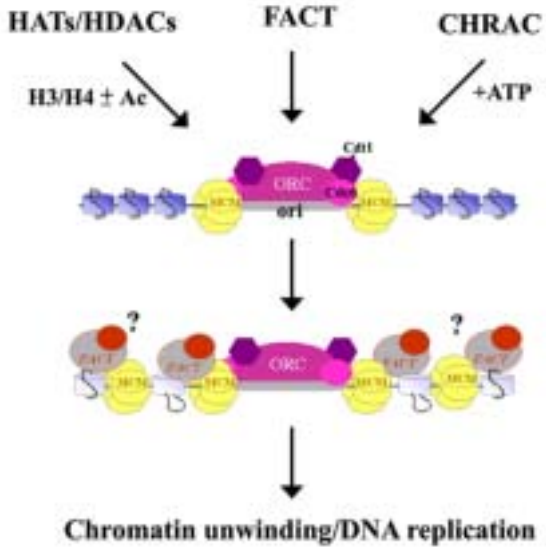
HATs/HDACs
FACT
CHRAC
H3/H4 ± Ac
+ATP
Cdt1
ORC
Cdc6
ori
?
?
ORC
Chromatin unwinding/DNA replication